2005-11-11

Piezoresistive Sensing of Bistable Micro Mechansim State

Jeffrey K. Anderson
Brigham Young University - Provo

PIEZORESISTIVE SENSING OF BISTABLE MICRO MECHANISM STATE

by

Jeffrey K. Anderson

A thesis submitted to the faculty of

Brigham Young University

in partial fulfillment of the requirements for the degree of

Master of Science

Department of Mechanical Engineering

Brigham Young University

December 2005

BRIGHAM YOUNG UNIVERSITY

GRADUATE COMMITTEE APPROVAL

of a thesis submitted by

Jeffrey K. Anderson

This thesis has been read by each member of the following graduate committee, and by majority vote has been found to be satisfactory

Date	Larry L. Howell, Chair
Date	Timothy W. McLain
Date.	Brian D. Jensen

BRIGHAM YOUNG UNIVERSITY

As chair of the candidates's graduate committee, I have read the thesis of Jeffrey K. Anderson in its final form and have found that (1) its format, citation, and bibliographic style are consistent and acceptable and fulfill university and department style requirements; (2) its illustrative materials including figures, tables, and charts are in place; and (3) the final manuscript is satisfactory to the graduate committee and is ready for submission to the university library.

Date

Larry L. Howell
Chair, Graduate Committee

Accepted for the Department

Matthew R. Jones
Graduate Coordinator

Accepted for the College

Alan R. Parkinson
Dean, Ira A. Fulton College of Engineering and Technology

ABSTRACT

PIEZORESISTIVE SENSING OF BISTABLE MICRO MECHANISM STATE

Jeffrey K. Anderson

Department of Mechanical Engineering

Master of Science

The objective of this work is to demonstrate the feasibility of on-chip sensing of bistable mechanism state using the piezoresistive properties of polysilicon, thus eliminating the need for electrical contacts. Changes in position are detected by observing changes in resistance across the mechanism. Sensing the state of bistable mechanisms is critical in their various applications. The research in this thesis advances the modeling techniques of MEMS devices which use piezoresistivity for position sensing.

A fully compliant bistable micro mechanism was designed, fabricated, and tested to demonstrate the feasibility of this sensing technique. Testing results from two fabrication processes, Fairchild's SUMMiT IV and MUMPs, are compared. The Fairchild mechanism was then integrated into various Wheatstone bridge configurations to show the advantages of bridges and to demonstrate various design layouts. Repeatable and detectable results were found with independent mechanisms and with those integrated into Wheatstone bridges.

Finite element models were constructed for the different Wheatstone bridges which were used to predict piezoresistive trends. A bistable mechanism for high-acceleration sensing was designed using uncertainty analysis optimization. The piezoresistive effects for this mechanism were also modeled. Discussion concerning nonvolatile memory applications is also presented.

ACKNOWLEDGEMENTS

I would like to thank my graduate committee for their time spent in my behalf: Dr. Howell, Dr. McLain, and Dr. Jensen. Dr. Howell's help was invaluable, and it has been a great privilege working under his direction. Fellow graduate students Jon Wittwer and Rob Messenger have provided help in many different ways. Jon Wittwer's expertise was particularly necessary in bistable mechanism design and uncertainty optimization.

Thanks need to be given to my family for their encouragement over the years. Special recognition should be given to my wife, Emily, who has loved and supported me through it all.

Funding from National Science Foundation grant number CMS-0428532 made this research possible. Thanks to BlockMEMS for providing the Fairchild parts for testing and to Sandia National Laboratories for inviting me to use their facilities for the testing portion of this thesis.

TABLE OF CONTENTS

LIST OF FIGURES

LIST OF TABLES

CHAPTER 1 INTRODUCTION

1.1 Objective

The objective of this work is to demonstrate the feasibility of on-chip sensing of bistable mechanism state using the piezoresistive properties of polysilicon, thus eliminating the need for electrical contacts. Changes in the position of the device are detected by observing changes in resistance across the mechanism. The resistance change occurs due to the change in internal stress experienced as the mechanism switches position. By reading the resistance across the bistable mechanism, position can be determined and device reliability will be increased.

Piezoresistive sensing with bistable mechanisms can be demonstrated through testing performed on devices that were analyzed, designed, and fabricated as part of this research. The advantages of measuring resistance using a Wheatstone bridge will also be shown. Finite element analysis (FEA) can be used to predict the mechanical and resistive behavior of the bistable mechanism throughout its motion, and such an FEA model will be used in this thesis. Possible applications will also be investigated and discussed to demonstrate the need for this sensing technology.

1.2 Motivation

The use of compliant mechanisms in microelectromechanical systems (MEMS) reduces significant uncertainty associated with tolerances, backlash, friction, and wear. Other sources of uncertainty, such as material properties, manufacturing process variation, and stiction, can have large effects on compliant MEMS. The flexural modulus can be dra-

matically altered by different grain orientations in the material, and small variations in dimensions and layer thicknesses can cause mechanisms to deviate from their ideal behavior. In bistable mechanisms, this deviation can even introduce uncertainty in the position of the mechanism. A sensing technique is thus required to detect the mechanism's position and insure device reliability.

The integration of sensors into micro devices poses significant challenges because the sensors are often orders of magnitude larger than the mechanisms being monitored. Large sensing apparatus petitions the practicality and applicability of micro devices. Piezoresistive position sensing utilizes inherent properties of mechanisms to accurately determine device position with minimal space requirements. The sensing components may resultantly be smaller than their targeted device. When combined with MEMS devices, these small sensors increase the design freedom felt by MEMS designers by allowing devices to be designed without drastic alterations for sensor integration. Piezoresistive position sensing can be combined with various micro mechanisms to provide accurate and necessary position information.

Sensing the state of bistable mechanisms is critical in their various applications, such as nonvolatile memory or high-acceleration sensing arrays. Detecting the state of the bistable device is essential in these applications. Commonly, electrical contacts are used to determine the state of a mechanism by using the mechanism to close an electrical circuit. This new circuit formation is detected, and the mechanism's position is deduced. Piezoresistive position sensing eliminates reliability issues and errors associated with electrical contacts by completely eliminating the contact. On-chip sensing is integrated into the device design, and very low power is required to sense changes in mechanism position.

1.3 Contributions

The research in this thesis advances the modeling techniques of MEMS devices which use piezoresistivity for position sensing. Models were developed using finite element analysis to predict the resistive behavior of the bistable mechanisms. FEA has been used to model piezoresistive changes in resistors with simple geometries, but this thesis presents methods which use mechanisms with more complex geometries as resistive ele-

ments. Possible applications are presented to further the commercialization of this technology. The ability to determine the position of a bistable mechanism in the simple manner presented in this thesis contributes to the reliability and performance of this and similar MEMS devices.

1.4 Document Organization

The next chapter provides background for the technology, including a literature review. The remainder of the thesis is found in two main parts which are included as Chapters 3 and 4. Chapter 3 describes the modeling, design, testing, and results of the fully compliant bistable micromechanism with piezoresistive position sensing. Possible applications and designs for these applications are discussed in Chapter 4. Chapter 3 is drawn from a paper that was being prepared for publication at the time this thesis was written. The format of this chapter allows it to be read independent of the rest of the thesis, while the abstracts, references, and appendices have been consolidated with those of the thesis.

CHAPTER 2 BACKGROUND

2.1 MEMS

Microelectromechanical systems (MEMS) consist of mechanisms and electrical components with feature sizes ranging from micrometers to millimeters [1].

MEMS are manufactured using processes similar to those utilized in integrated circuit fabrication. In common methods, planar layers of polysilicon are deposited on a substrate and are alternated with sacrificial silicon oxide layers. Individual layers are created using chemical vapor deposition (CVD). Each polysilicon layer is patterned using planar lithography before the next layer is deposited. This patterning allows the creation of geometries, the joining of multiple layers, and the anchoring of mechanisms to the substrate. The number of usable layers depends on the specific manufacturing process. Two releasable layers are used in the Multi-User MEMS Process (MUMPS) while up to four layers are utilized by Sandia's SUMMiT V process. The final step of the manufacturing process is the chemical release of the embedded polysilicon layers. The sacrificial silicon oxide layers are etched away, freeing the remaining mechanisms and facilitating mechanism motion. Several different manufacturing methods are used with varying techniques [2][3].

2.2 Compliant Mechanisms

Compliant mechanisms obtain at least some of their mobility from the deflection of flexible members. Systems that undergo large amounts of deflection cannot accurately be analyzed using linear deflection methods.

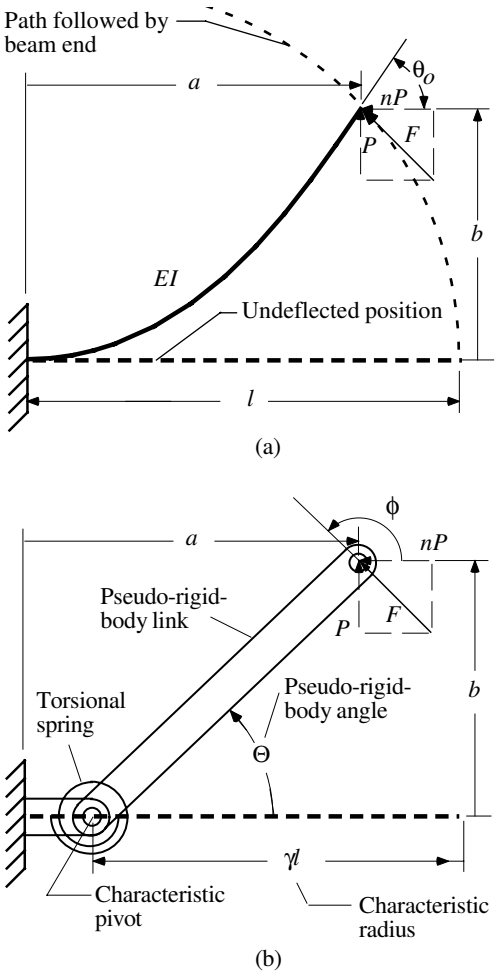

Figure 2.1: (a) Cantilevered segment with forces at free end, and (b) its pseudo-rigid-body model [1].

The pseudo-rigid body model (PRBM) provides a simplified method of analyzing nonlinear kinematic systems. The PRBM uses rigid-body components with equivalent force-deflection characteristics to model flexible members, as is shown in Figure 2.1 for a cantilever beam with forces at the free end. Rigid-link mechanism theory can then be used to analyze the compliant mechanism [1]. A fully compliant mechanism is defined as a mechanism that gains all of its motion from the deflection of flexible members (i.e. no motion is gained from pin joints or sliders).

Some geometries, such as pin joints, are difficult to create using the layered processes of micromechanism fabrication. Manufacturing variation, joint clearances, and part friction contribute to non-ideal performance in mechanisms which utilize such geometries.

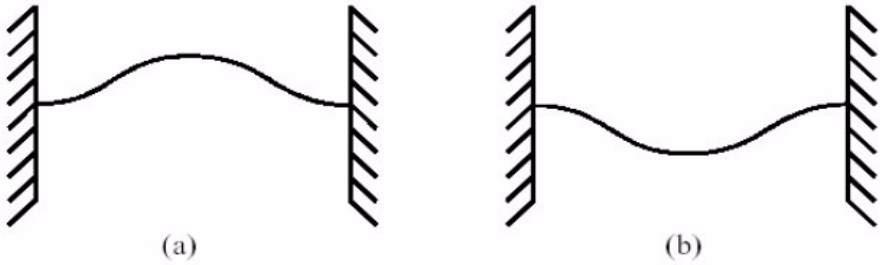

Figure 2.2: A snap-through buckling mechanism in both stable equilibrium positions [4].

Compliant mechanisms are an ideal application for MEMS, because complex, reliable devices can be manufactured using existing methods.

2.3 Bistable Mechanisms

A bistable mechanism is a device that tends toward one of its two stable equilibrium positions [5]. The mechanism will then remain in this position without any external force. Common examples of bistable mechanisms are light switches, three-ring binders, and plastic bottle lids. Opdahl [9][10] presents a classification method which allows the characterization of various bistable mechanisms. Snap-through buckling mechanisms are best suited for piezoresistive position sensing because there are no breaks in electric contact and there is a large difference in stress present in the mechanism between the first equilibrium position and a stopped, second stable position. Snap-through buckling in both stable equilibrium positions is illustrated in Figure 2.2.

Compliant mechanisms demonstrate bistability when there are two minima on the potential energy vs. displacement curve. This concept can be demonstrated using the ball-on-the-hill analogy shown in Figure 2.3. The local minima of the curve (positions A and D) are the two stable equilibrium positions. A force applied to the ball at either of these positions would cause the ball to oscillate and return to its original position. Position B is the unstable equilibrium position where a slight input of energy in either direction will result in the ball rolling to one of the stable positions. The stop shown in position C has created a new, externally constrained, stable equilibrium position. A neutrally stable condition (position E) exists when an input force will cause the ball to move to a new dis-

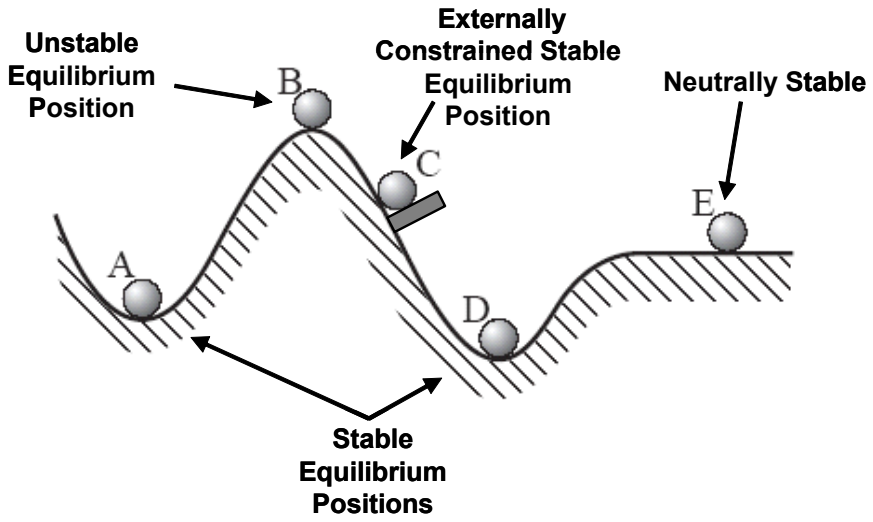

Figure 2.3: Ball-on-the-hill analogy of bistable mechanisms.

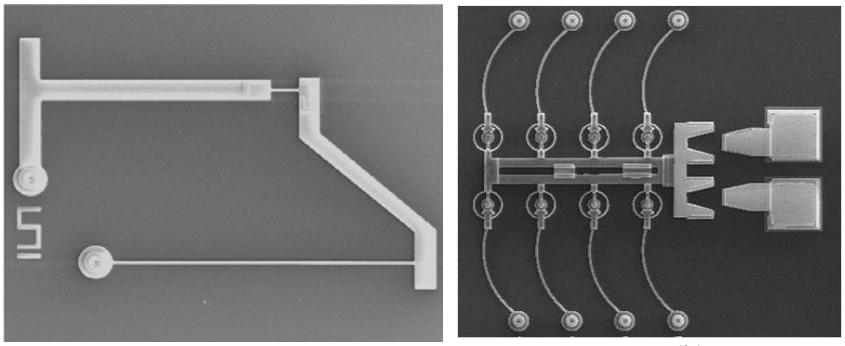

(a) (b)

Figure 2.4: Partially compliant micro bistable mechanisms (a) Young mechanism [11] and (b) linear-displacement bistable mechanism [12].

turbed position. The ball-on-the-hill analogy represents the potential energy vs. displacement curve of a particular bistable mechanism.

The Young mechanism is a partially compliant bistable mechanism which can be modeled as a four-bar rigid-link mechanism using the Pseudo-Rigid-Body Model. Young mechanisms contain two pin joints and undergo rotary motion [11]. Initially curved, pinned-pinned segments make up the legs on the linear-displacement bistable mechanism [12]. These partially compliant bistable mechanisms are shown in Figure 2.4.

The fully compliant bistable mechanism (FCBM) contains no pin joints, gaining all motion from the deflection of flexible members [5]. The FCBM uses a central shuttle to constrain its motion to linear displacement. Wittwer et. al. [13] presented a fully compliant bistable mechanism that eliminated the need for flexible, vertical members.

Fully compliant bistable mechanisms have also been designed with self-retracting capabilities by using thin, tensoral segments [15]. After the mechanism has snapped to its second stable equilibrium position, a voltage is applied across the mechanism. This voltage heats the tensoral segments which moves the energy curve such that the mechanism is no longer bistable. The mechanism then snaps back to its only stable position.

2.4 Piezoresistive Sensing

Piezoresistance and piezoresisitivity describe resistance changes due to induced stress. Piezoresistance is more general and refers to the change in resistance R. Piezoresistivity refers to the material property, ρ, which can change due to mechanical stress. The two properties are related by the equation

$$R = \rho \frac{l}{wh} \qquad \text{Eq. 2.1}$$

where l, w, and h, are geometric dimensions of the resistor (equation assumes a rectangular cross-section).

Piezoresistivity has also been used to determine the position of a thermal in-plane micro actuator (TIM) and provide data for feedback control [28][29]. Displacement measurements were captured by piezoresistive position sensing and used in feedback control of the TIM.

CHAPTER 3 PIEZORESISTIVE SENSING OF BISTABLE MICRO MECHANISM STATE

3.1 Introduction

The objective of this work is to demonstrate the feasibility of on-chip sensing of bistable mechanism state using the piezoresistive properties of polysilicon. Two approaches are proposed and demonstrated: 1) sensing the resistance change in the mechanism caused by the strain in the second equilibrium position, and 2) integrating the mechanism in bridge configurations for increased sensitivity in determining resistance changes. Four different bridge configurations are investigated. Sensing the state of bistable mechanisms is critical in their various applications, such as nonvolatile memory or high-acceleration sensing arrays. The proposed approach allows on-chip state sensing with a potential of dramatic increase in reliability.

Electrical contacts are often used to determine the state of a mechanism by using the mechanism to close an electrical circuit in one of its states. However, tolerances and fabrication variation lead to challenges with electrical contacts. Contact resistances can vary across a wafer and change between operating cycles. Polysilicon is a poor contact material because it is too hard, and its resistivity is too high. This work proposes piezoresistive position sensing to eliminate reliability issues and errors associated with electrical contacts by completely eliminating the contact. On-chip sensing is integrated into the device design, and very low power is required to sense changes in mechanism position.

Measurable changes in resistance are required to detect the change in mechanism state. However, several challenges exist that complicate the problem. The magnitude of the resistance change is dependent on device design, material properties, and fabrication

process. The largest challenge is related to the fact that the sign of the resistance change in the mechanism is dependent on the direction of stress (tensile or compressive). Many MEMS devices use the piezoresistive effect on one surface of a membrane, which will be in tension or compression when under pressure. However, a beam in bending experiences both tensile and compressive stresses. The different signs of resistance change for compressive and tensile strain can combine to minimize the output signal or eliminate any detectable piezoresistive effect. Several devices are presented that address this challenge and make it feasible to use the piezoresistive properties of a bistable device to detect its state.

The background associated with bistable mechanisms and piezoresistive sensing is provided next. Testing on bistable mechanisms manufactured in Fairchild's SUMMiT IV process and MUMPs is then presented. Four bridge configurations were then tested to investigate potential advantages. Models predicting the trends of resistive behaviors are also presented.

3.2 Background

A bistable mechanism is a device that can toggle between two stable equilibrium positions [5]. The mechanism will then remain in this position without any externally applied force. Compliant bistable mechanisms can be used in many applications including switches [6], valves [7], and relays [8]. The application of compliant micro bistable mechanisms is of interest because the mechanism will remain in either position without requiring input power to maintain the position.

Opdahl [10] presents a classification method which allows the characterization of various bistable mechanisms. Snap-through buckling mechanisms are well-suited for piezoresistive position sensing because there are no breaks in electric contact and there is a large difference in stress present in the mechanism between the first equilibrium position and a stopped, second stable position. A stop is used to increase the amount of stress in the second stable position, facilitating a larger stress difference between the two measured positions.

Figure 3.1 shows a plot of the applied force vs. displacement curve for a bistable mechanism. This curve is the derivative of the energy curve with respect to displacement.

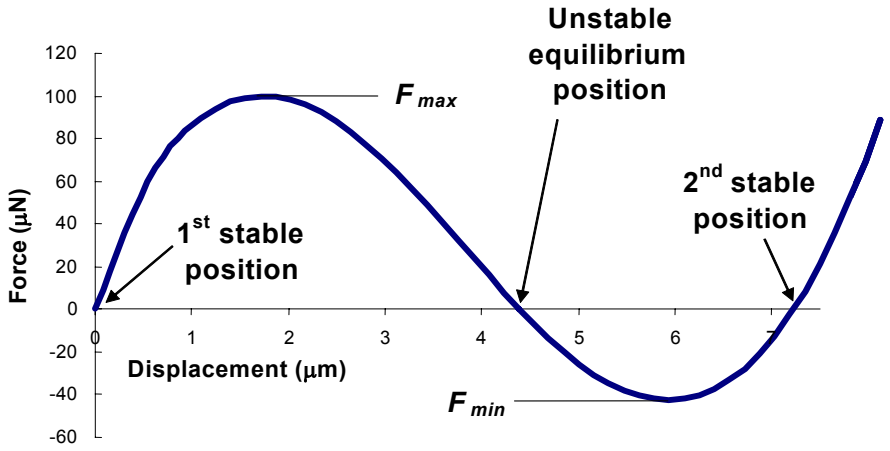

Figure 3.1: Typical force vs. displacement curve of a bistable mechanism.

The roots of the curves represent the peaks and valleys of energy, or the stable and unstable equilibrium positions. The switching forces can be determined by the magnitude of the maximum and minimum of the curve. If the bistable mechanism is to be used for an electrical contact, a stop can be placed at the minimum of the curve (around 6 μm in Figure 3.1) to maximize the contact force (thus reducing the contact resistance).

The fully compliant bistable mechanism (FCBM) contains no pin joints, gaining all motion from the deflection of flexible members [5]. The FCBM uses a central shuttle to constrain its motion to linear displacement. The FCBM topology used in this research was presented by Wittwer et al. [13] as shown in Figure 3.2.

Qiu [14] describes the advantages of a centrally clamped parallel beam bistable mechanism. Two parallel beams are connected in the center to insure that the buckling of the bistable mechanism is symmetric. This symmetric buckling mode can also be accomplished by the use of multiple sets of legs with a central shuttle (as in the FCBM). The shuttle acts as a central clamp, allowing the legs to move in parallel.

Variability in performance is introduced in micro mechanisms through joint clearances, friction forces, stiction, dimensional variations, and uncertain material properties [16]. Variability due to joint clearances can be eliminated by using a fully compliant bistable mechanism, but the behavior of the device shown in Figure 3.2 is still subject to

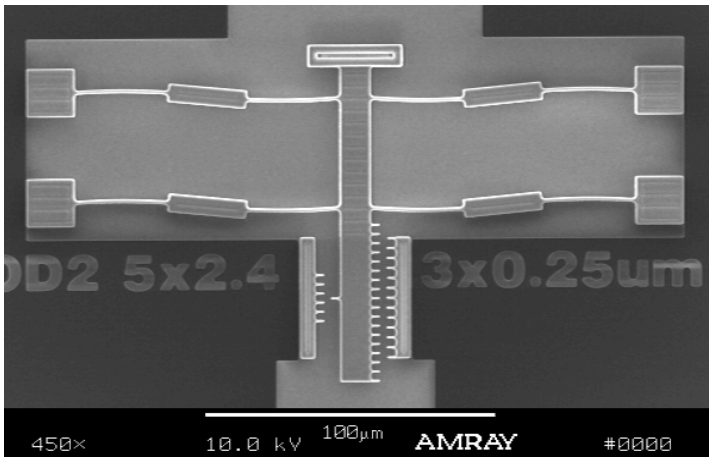

Figure 3.2: Fully compliant micro bistable mechanism in second stable equilibrium position [13].

variation in beam widths and residual stress [13]. The FCBM can be fabricated in a plane, making it practical for MEMS applications in which silicon or polysilicon is used as the structural material. Both silicon and polysilicon have been shown to be piezoresistive materials.

Piezoresistivity describes an effect in which the bulk resistivity is influenced by the mechanical stress applied to the material. This effect in silicon was described by Smith [17]. Semiconductor strain gauges utilizing this material property are two orders of magnitude more sensitive than metal gauges [18]. Changes in conductivity under stress are attributed to the raising and lowering of conduction band minima [19]. Warping of the band structure is also present in p-type silicon, yielding both a transfer of carriers and a change in effective mass [20].

Mathematical models have been developed to characterize changes in resistivity [21]. French and Evans developed a model, including the effects of grain boundaries, which describes the piezoresistive behavior of polysilicon [22] [23] [20].

Pressure sensors are a common application for piezoresistivity in polysilicon [19] [24] [25] [18]. Pressure sensing membranes are used in combination with specially-doped resistive areas. The resistors are deposited on top of the membrane and are in either compression or tension, depending on the direction of membrane deflection. In contrast, this work uses the entire mechanism as the resistive element, and in-plane motions are being measured instead of out-of-plane deflections.

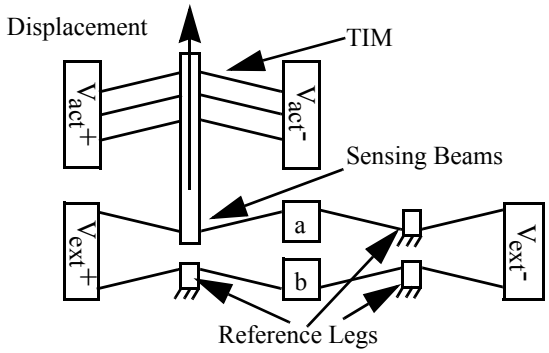

Figure 3.3: Piezoresistive position sensing setup for feedback control of a thermal actuator [28].

The effect of piezoresistivity has also been used to detect acoustic waves in a microphone [26] and to detect forces in the cantilevers of atomic force microscopes [27].

Piezoresistivity has been used to determine the position of a thermomechanical in-plane microactuator (TIM) [29][28]. Displacement measurements were captured by piezoresistive position sensing and used in feedback control of the TIM. The measurement setup is shown in Figure 3.3. Sensing beams were attached to the shuttle of the thermal actuator. The sensing beams then acted as resistors in a Wheatstone bridge, with both the sensing legs and the other resistors reflecting the geometry of a single set of actuator legs. As the TIM changed position, it deflected the sensing beam. This deflection induced stress, which changes the resistance of the sensing beam and the output of the bridge. The position was determined by the change in resistance, and the input signal to the TIM could be adjusted.

While the piezoresistive properties of mono crystalline silicon are generally well-understood and well-documented, polysilicon properties are more obscure and are complicated by process dependencies and variations. Values for the material bulk resistivity, ρ, and the piezoresistive matrix coefficients, π_{ij}, are used for finite element modeling. Symmetry conditions reduce the matrix to include only π_{11}, π_{12}, and π_{44}. The matrix coefficients are sensitive to crystal orientation, doping type, doping level, and operating temperature [30]. Smith [17] reports the resistivity and matrix coefficients for mono crys-

talline n- and p-type silicon. It is predicted that polysilicon has a large, negative π_{11} value, a π_{12} value of the opposite sign and half the magnitude, while π_{44} is predicted to be zero [19]. French and Evans [20] report averaged π_l and π_t (longitudinal and transverse) values for polysilicon over 5 planes plus random orientation structure. Gridchin and Lubimsky [31] provide formulas to calculate polysilicon matrix coefficients for different crystal orientations from the mono crystalline values.

Accurate values for π_{11}, π_{12}, and π_{44} are not currently available for the polysilicon used because these material properties have not been accurately characterized. Fortunately, the primary objective of this work is to demonstrate that bistable mechanism state can be determined using the piezoresistive effect. The models developed in the work are meant to predict trends, and the piezoresistive properties published by Smith [17] for n-type silicon are found to be adequate for this purpose. It was shown that the modeling results with these values show the important trends and give a conservative estimate of most experimental measurements. The values used for the modeling in this paper are listed in Table 3.1.

Table 3.1: Piezoresistive values used for FEA modeling.

ρ (T$\Omega\mu$m)	11.7e-8
$\pi_{11}(MPa)^{-1}$	-102.2e-5
$\pi_{12}(MPa)^{-1}$	53.4e-5
$\pi_{44}(MPa)^{-1}$	-13.6e-5

Piezoresistive position sensing is advantageous due to the small size of the sensing mechanism. Capacitive sensing is commonly used in sensing changes in mechanism position (e.g. as seen in accelerometers). Hälg [32] designed a bistable beam with capacitive sensing capabilities. The beam was electrostatically actuated and would remain in either position for an indefinite amount of time. A limitation of capacitive sensing is the very small change in capacitance that is difficult to measure. Piezoresistive sensing uses much less space and can produce greater differences in signal when the bistable mechanism switches position. Data collection can be achieved using electrical probes or wire-bonding

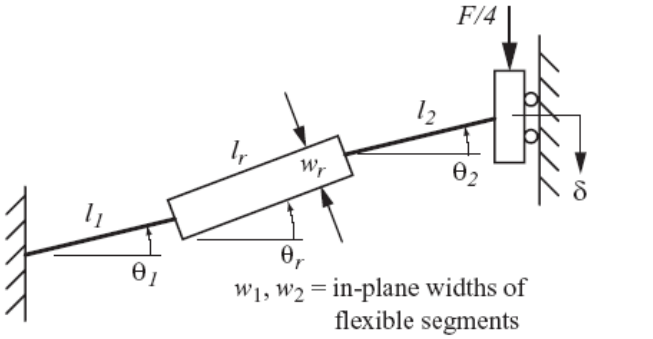

Figure 3.4: Design parameter description of the quarter-model of a fully compliant bistable mechanism [13].

circuitry as opposed to capacitive sensing, which usually requires on-chip circuitry. These capabilities make piezoresistive position sensing a feasible and promising alternative to capacitive sensing.

3.3 Devices without Bridge

The simplest possible configuration is to use the flexible elements of the bistable mechanism as the sensing elements, without a Wheatstone bridge or other device. This section investigates the ability to detect device position without the use of a Wheatstone bridge was demonstrated by testing devices fabricated using two different surface micro-machining processes, the Fairchild SUMMiT IV process and MUMPs. Testing of a few devices was performed to demonstrate feasibility, and this will lead to a discussion of the device combined in bridge configurations. A single bistable mechanism, fabricated using the Fairchild SUMMiT IV process, was tested for a measurable resistance change between stable positions. The design parameters for the fully compliant bistable micromechanism are shown in Figure 3.4. Values and design variables for the bistable micromechanism are listed in Table 3.2. The values represent dimensions as drawn for manufacturing using Fairchild's SUMMiT IV process (an additional 0.2 μm should be subtracted from the three width dimensions due to etch bias). The bistable mechanism tested had identical dimensions to the mechanisms later tested in bridge configurations. One mechanism was tested with five repetitions, and remote sensing was used to ensure accuracy of the applied

Table 3.2: Design variables and values.

Variable	Value
l_1 (μm)	21.6
w_1 (μm)	1.7
θ_1 (deg.)	7.0161
l_r (μm)	80.0
w_r (μm)	6.2
θ_r (deg.)	2.167
l_2 (μm)	21.6
w_2 (μm)	1.65
θ_2 (deg.)	2.039

current. Five levels of current were applied to the mechanism, and the voltage was measured in both positions. The results of this testing are shown in Table 3.3.

Table 3.3: SUMMiT voltage changes for mechanism without Wheatstone bridge.

	SUMMiT Mechanism	
I_{in} (mA)	ΔV (mV)	Std. Dev. (mV)
0.5	0.94	0.15
1.0	2.0	0.11
1.5	3.0	0.16
2.0	4.2	0.13
2.5	5.3	0.26

Bistable mechanisms produced in MUMPs [33] were also tested to determine the magnitude of the resistance change associated with the toggling of the mechanism's position. The design parameters for the fully compliant bistable micromechanism are shown in

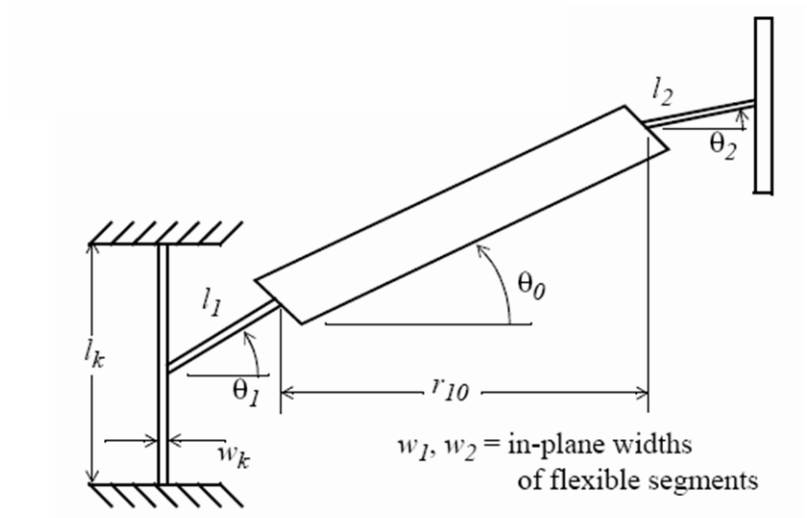

Figure 3.5: Design parameterization of MUMPs fully compliant bistable mechanism [5].

Figure 3.5. Values and design variables for the bistable micromechanism are listed in Table 3.4. Remote sensing was again used to ensure that the mechanism experienced the

Table 3.4: MUMPs design variables and values.

Variable	Value
l_1 (μm)	95.7
w_1 (μm)	2.5
θ_1 (deg.)	6.9
r_{10} (μm)	145.5
θ_0 (deg.)	6.1
l_2 (μm)	77.3
w_2 (μm)	2.5
θ_2 (deg.)	7.1
l_k (μm)	64
w_k (μm)	3.5

desired applied current. Three identical bistable mechanisms were measured on two separate die. Each mechanism was measured five times in both stable positions. The measurements for the MUMPs bistable mechanisms are listed in Table 3.5. The results for the two

Table 3.5: MUMPs voltage changes for mechanisms without Wheatstone bridge.

	MUMPs Mechanisms	
I_{in} (mA)	ΔV (mV)	Std. Dev. (mV)
0.5	4.9	0.25
1.0	9.7	0.48
1.5	14	0.91
2.0	18	1.7
2.5	21	3.0

mechanisms should be evaluated independently because they were fabricated by different processes, made with different material properties, and used different bistable mechanism designs. Detectable voltage changes were recorded for both mechanisms independent of bridge integration. In applications where mechanism size is critical, layouts could be used without Wheatstone bridge configurations.

While the resistance of the SUMMiT device remained constant throughout all input currents, a nonlinear trend (Figure 3.6) occurred in the resistance of the MUMPs device as the source current increased. The maximum standard deviation associated with these measurements was 1.1 ohms, demonstrating that the nonlinearity of the data points is larger than the standard deviation of the measurements. The nonlinearity of the mechanism's resistance could be attributed to the temperature change of the material as described by Gad-el-Hak [30]. This is reasonable, because a similar topology is used for thermal actuators, where resistivity is known to be affected by temperature [34]. This section demonstrates the feasibility of piezoresisti9ve sensing of bistable mechanism state using the flexible members of the bistable mechanism as sensing elements. This simple

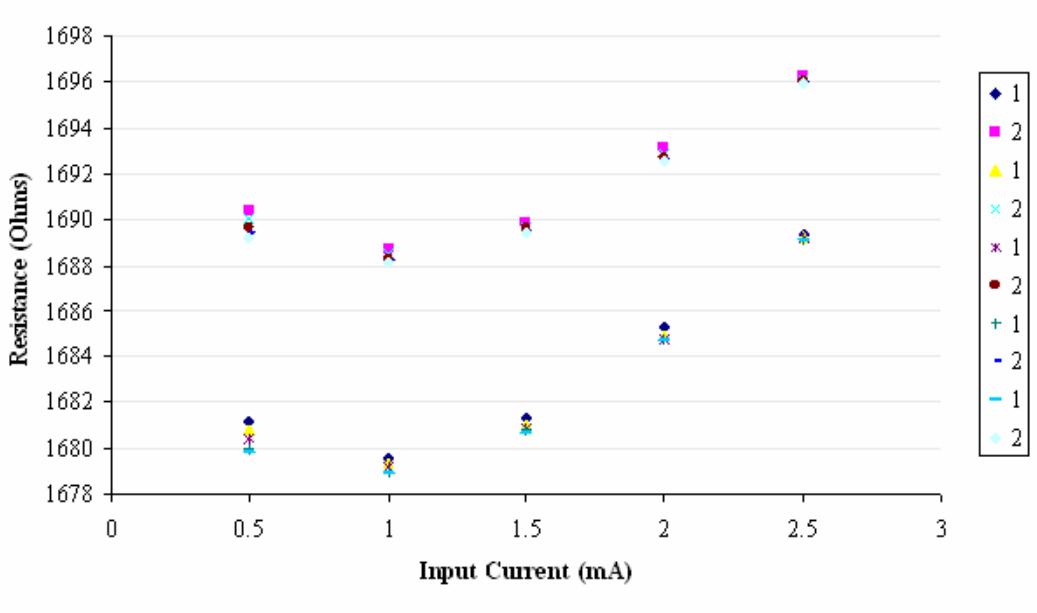

Figure 3.6: Resistance change with current of MUMPs bistable mechanism.

approach leads to the investigation of devices integrated in a Wheatstone bridge configuration, as described next.

3.4 System Device Design

Bistable mechanisms were fabricated in Wheatstone bridge configurations, where mechanisms with the same dimensions described in Table 3.2 were used as resistors in the bridges. Figure 3.7 displays the four fabricated configurations with assigned labels A through D.

Configuration A (Figure 3.7 (a)) uses a quarter bridge configuration with all four resistors made of identical bistable mechanisms. The identical mechanisms were used to ensure that the Wheatstone bridge was balanced.

Figure 3.7 (d) (configuration D) shows a quarter bridge with two mechanisms and two beams elements. The beam elements were designed to have resistances similar to that of the bistable mechanism. The lower mechanism is physically stopped to prevent deflection under residual stress.

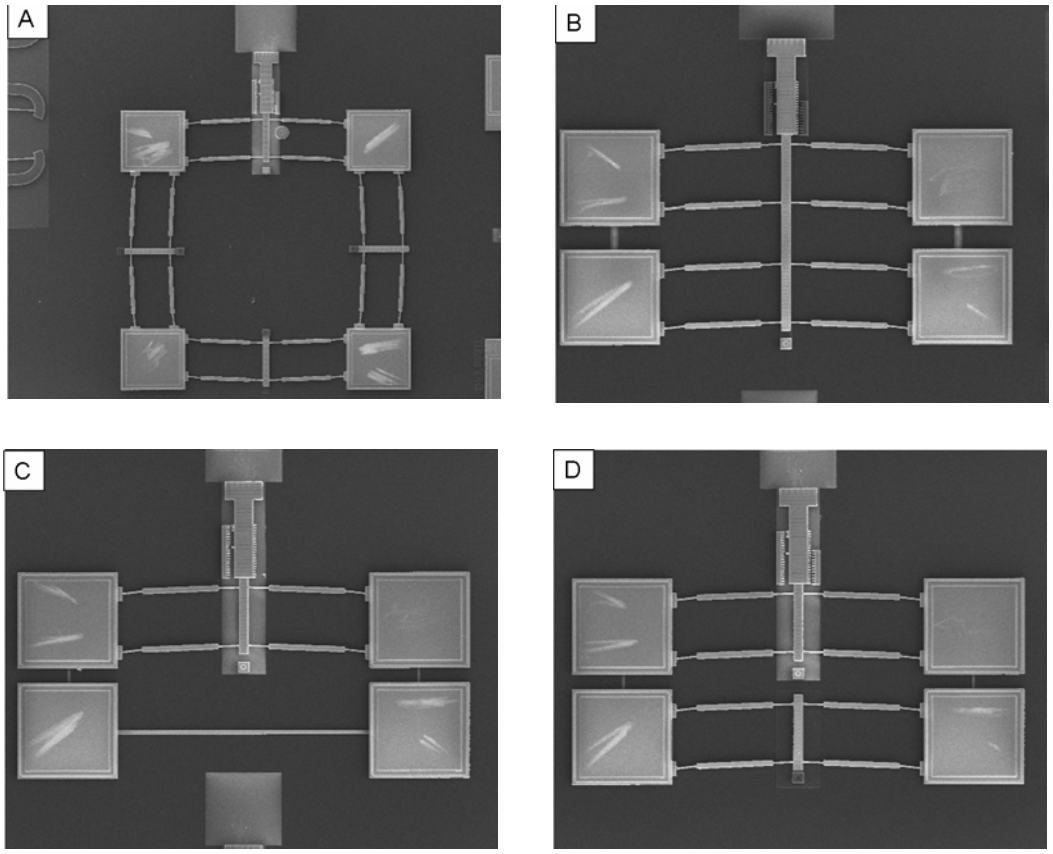

Figure 3.7: Four bistable mechanism bridge configurations.

Similar to configuration D, configuration B (Figure 3.7 (b)) uses two mechanisms and two beam resistors. The shuttles of the two mechanisms are connected in configuration B, allowing both mechanisms to toggle positions simultaneously. The potential of yielding a higher change in resistance between the two positions exists due to the resistive changes in two mechanisms, but electrical connection of the two shuttles alters the circuitry of the bridge.

A quarter bridge with three beam elements is shown in Figure 3.7 (c) (configuration C). This configuration could be designed to be the most compact, with stacked beams manufactured in different layers.

The dimensions of the beam resistors for each configuration are listed in Table 3.6, where configuration C has two values for the vertical and horizontal beam resistors. Each of these configurations was tested to determine the effects of the different Wheatstone bridge architectures.

Table 3.6: Beam resistor dimensions.

	Width (μm)	Length (μm)	Thickness (μm)
Configuration B	9.367	26.0	0.3
Configuration C (1)	2.989	16.0	0.3
Configuration C (2)	4.416	265.028	2.8
Configuration D	2.989	16.0	0.3

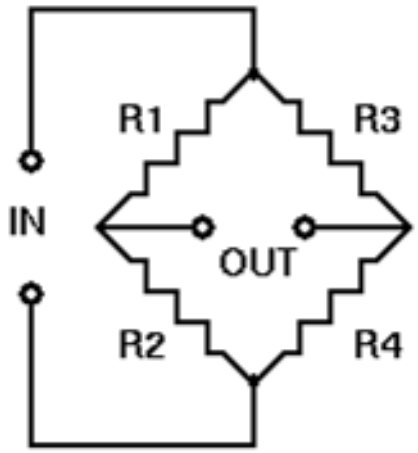

Figure 3.8: Wheatstone bridge schematic.

Wheatstone bridges are circuits designed to sense small changes in resistance (Figure 3.8). An input voltage is applied, and an output voltage is measured. For a balanced bridge (*R1/R2= R3/R4*), the output voltage will be zero for any input voltage. Balanced bridges mitigate temperature varying effects because all resistors in the bridge heat up at the same rate. The equation describing the output voltage is

$$Vo = Vi\left(\frac{R1}{R1+R2} \angle \frac{R3}{R3+R4}\right) \qquad \text{Eq. 3.1}$$

where V_o is the output voltage, and V_i is the source voltage. Quarter-bridge configurations were used in this research, where the bistable mechanism is the variable resistor. A change in *R1* (the resistance of the bistable mechanism) will change to some new value, *R1'*, where $R1' = R1 + \delta R$. The output from the bridge then is

$$Vo + \delta Vo = Vi\left(\frac{R1'R4 \angle R3R2}{(R1' + R2)(R3 + R4)}\right) \quad \text{Eq. 3.2}$$

For a balanced, quarter bridge circuit, the voltage change can be simplified to contain a single resistance, *R*, such that

$$\Delta V = \frac{\Delta R}{4R} Vi \quad \text{Eq. 3.3}$$

Wheatstone bridges are used in this research in order to detect small changes in the resistance of a bistable mechanism. The resistance of the SUMMiT bistable mechanism used in this work was measured to be 90.7 ohms with a standard deviation of 1.03 ohms. The change in resistance detected when the mechanism toggles positions was found to be 2.0 ohms with a standard deviation of 0.17 ohms. Table 3.7 shows the voltage changes predicted by Equation 3.3 at three voltage source levels for a balanced quarter-bridge (configuration A) using these measured resistive values.

Table 3.7: Predicted voltage changes for configuration A.

V_s (Volts)	ΔV (mV)
0.5	2.77
1.0	5.53
1.5	8.30

The simple model of Equation 3.3 was a good prediction of actual device behavior for configuration A (see Table 3.8). Due to balance in the bridge and identical resistors, configuration A should be insensitive to variations in temperature. Temperature changes in the bridge will be experienced equally among all resistors. Configurations C and D are quarter bridge configurations but may not be balanced due to the use of beams as resistors. These configurations will thus be more sensitive to temperature variations, and Equation 3.3 will be less accurate in predicting device behavior. Configuration B is not a Wheatstone bridge due to the connection of the central shuttles, and its behavior cannot be predicted using simple equations.

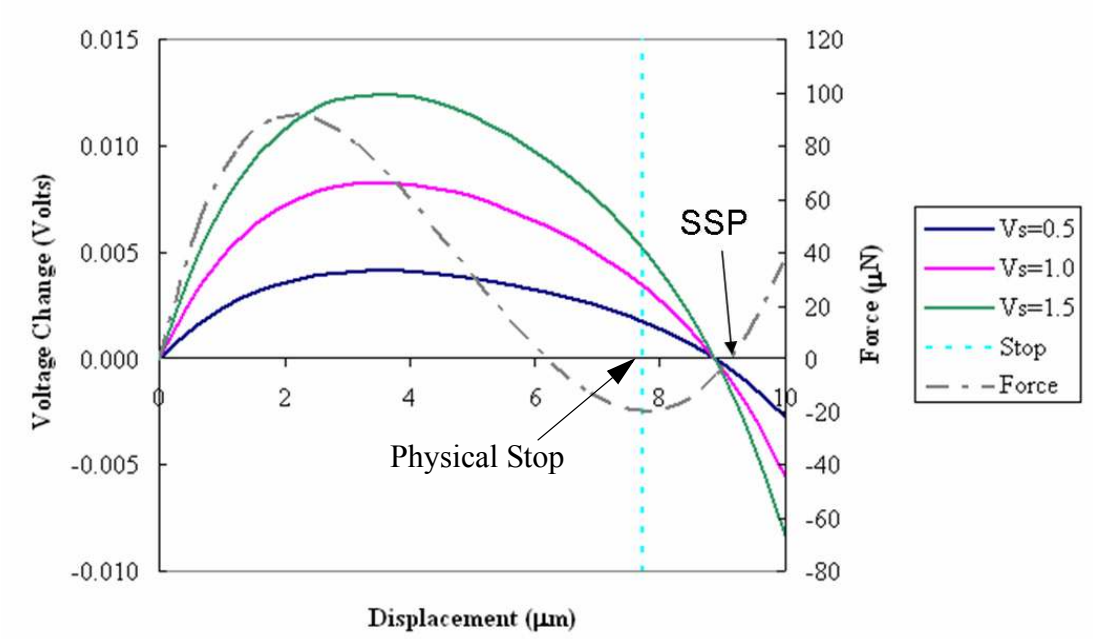

Figure 3.9: Configuration C modeling results.

3.5 Modeling

Finite element analysis was performed using ANSYS to model each configuration. Two-dimensional, coupled-field, piezoresistive elements (PLANE223) were used to predict the structural and piezoresistive properties of the polysilicon devices. All four layouts were modeled in their bridge configurations, with source voltages applied and output voltages measured. The results for all configurations were similar, with the results of configuration C shown in Figure 3.9. Voltage changes for three source voltages are shown as solid lines. The force-displacement plot (dashed line) of the bistable mechanism is displayed on the secondary axis for position reference. The vertical line indicates the position of the physical stop used to hold the second stable position at a state of higher stress. The importance of the stop can be seen by observing the small voltage changes when the mechanism reaches its natural, second stable equilibrium position (SSP). Experimental data reflects the point where each voltage curve intersects the vertical line, i.e. the voltage change between the as-fabricated position and the switched, stopped position.

3.6 Testing and Results

Ten different modules were tested, with one instance of each configuration per module. Seven of the modules were tested using probes (module numbers 1-7), while three modules were wire-bonded to obtain better electrical contacts (numbers 8-10).

Probe Testing

Two Keithley 2400 Digital SourceMeters were used to power the bridge and measure the output voltage utilizing seven probes. The first SourceMeter was used exclusively to apply an accurate voltage to the bridge. Four probes were used in the four-sense mode (remote sensing) to power the bridge. Two probes apply the source voltage, while two neighboring probes read the voltage to insure the application of the desired voltage level. When the source voltage is detected to vary from the desired level, the SourceMeter increases or decreases the applied power to insure that the device experiences the correct voltage. The wires connecting the power source to the probes and the interface between the probes and the bond pads introduce resistive losses into the system. This is especially important with devices fabricated using the Fairchild SUMMiT IV process, because bond pads are not metallized. The four-wire sense mode mitigates the effects of these resistive losses, and facilitates the accurate application of the source voltage. The second SourceMeter is used as a voltmeter to measure the output voltage of the bridge. A seventh probe is used for mechanism actuation. This setup is shown in Figure 3.10 for configuration B. A similar setup was used with other configurations. Each configuration was tested at three excitation voltages: 0.5, 1.0, and 1.5 volts. Three measurements were taken with the bistable mechanism in its first position (one at each excitation voltage). The mechanism was toggled, and three more measurements were recorded in the second stable position. This sequence was repeated five times for each mechanism across the seven probe-tested modules. The power source was turned off between each measurement, and the probes adjusted to optimize the output signal.

The non-metallized bond pads of the tested devices limited the precision of the measurements. The output on the voltmeter would converge on a value after the probes were adjusted to yield better contacts. Once the output converged, the results were repeat-

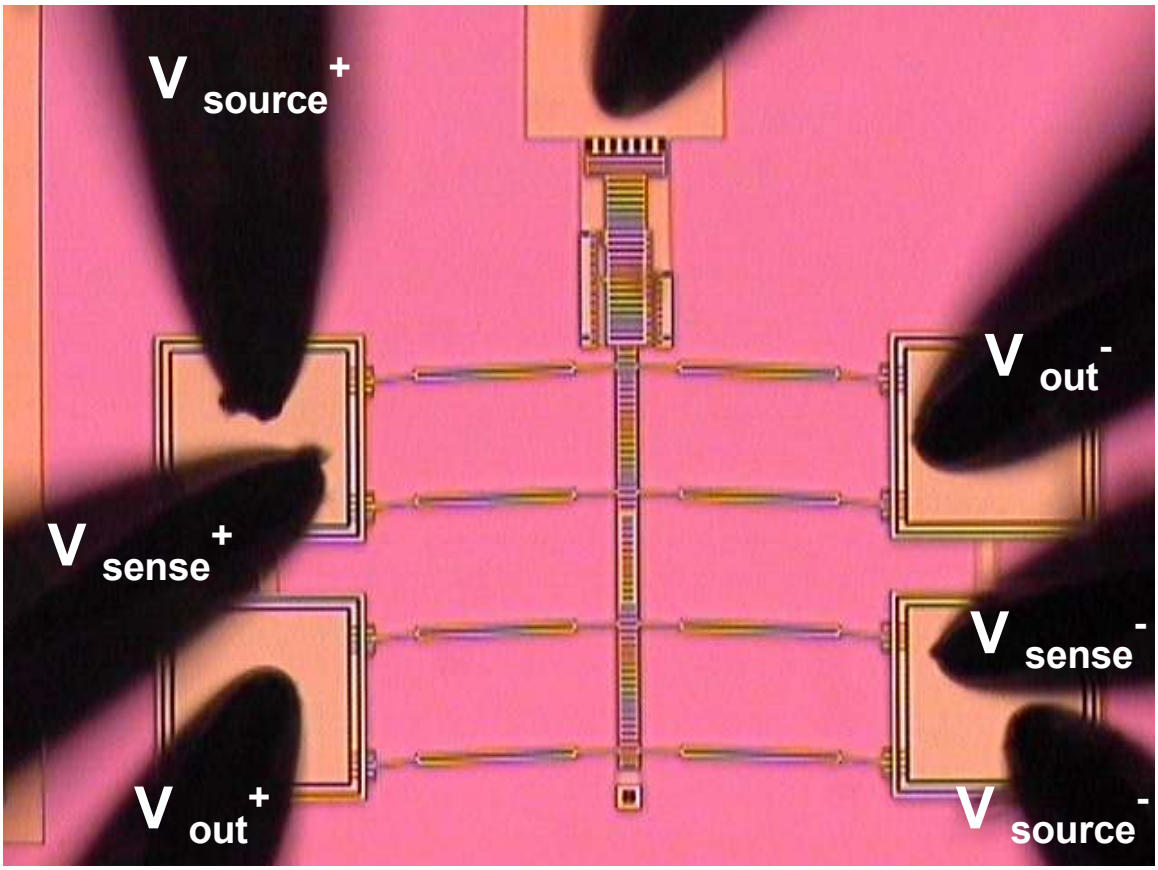

Figure 3.10: Probe setup for piezoresistive position testing.

able. Measurements were taken with 0.0001 volt precision. The Keithley 2400 is capable of more precise measurements, but the precision was limited by the quality of the resistive probe-bond pad contacts.

Wire-Bonded Testing

In order to reduce measurement error due to contact resistance and other resistive losses, three modules were wire bonded. Remote sensing could not be used because the bond pads were only large enough for one wire. Aluminum wire was used to bond the pads to the module carrier. The procedures described for probe testing were used to obtain measurements, but four-wire remote sensing could not be used. The same three excitation voltages were used, and each mechanism was measured five separate times in both positions at each excitation voltage. As expected, the output voltage was very steady, showing

no signs of deviation. The use of wire-bonding also allowed measurements to be taken with an additional decimal place of accuracy.

Results

Each configuration experienced a measurable change in voltage when the bistable mechanism position was toggled. The measured voltage changes are shown in Figure 3.11. Data is missing for modules where devices were damaged or electrically grounded. Configuration B showed the largest change in voltage between the two positions, while all configurations yielded consistent results with small variation. This is expected in configuration B since it has two active sensing legs. Configurations C and D had very similar results, but exhibited the smallest change in output voltage. Intermediate changes were experienced by configuration A. The measurements of the wire-bonded parts exhibited smaller variation with voltage changes similar to those seen with the probe-tested modules. Measured average voltage changes, standard deviations, and the model predictions (ΔV_M) are shown in Table 3.8 for each configuration and source voltage level. The magnitudes of the voltage changes are large enough to be easily measured.l

Table 3.8: Voltage changes, standard deviations, and model predictions (mV).

	Configuration A			Configuration B			Configuration C			Configuration D		
V_s (Volts)	ΔV	Std. Dev.	ΔV_M	ΔV	Std. Dev.	ΔV_M	ΔV	Std. Dev.	ΔV_M	ΔV	Std. Dev.	ΔV_M
0.5	2.8	0.18	4.5	3.6	0.20	1.9	2.2	0.11	1.7	2.2	0.11	1.7
1.0	5.9	0.19	9.0	7.4	0.32	3.7	4.5	0.18	3.4	4.4	0.22	3.4
1.5	9.1	0.16	13	11	0.46	5.6	6.7	0.32	5.2	6.6	0.31	5.2

The models for configurations B, C, and D under-predict the voltage change, whereas the model over-predicts the signal for configuration A. The models for configurations C and D predict approximately 80% of the experimentally- obtained voltage change. The discrepancy between the model predictions and the measured values is believed to be primarily due to the inaccurate piezoresistive coefficients used in the models.

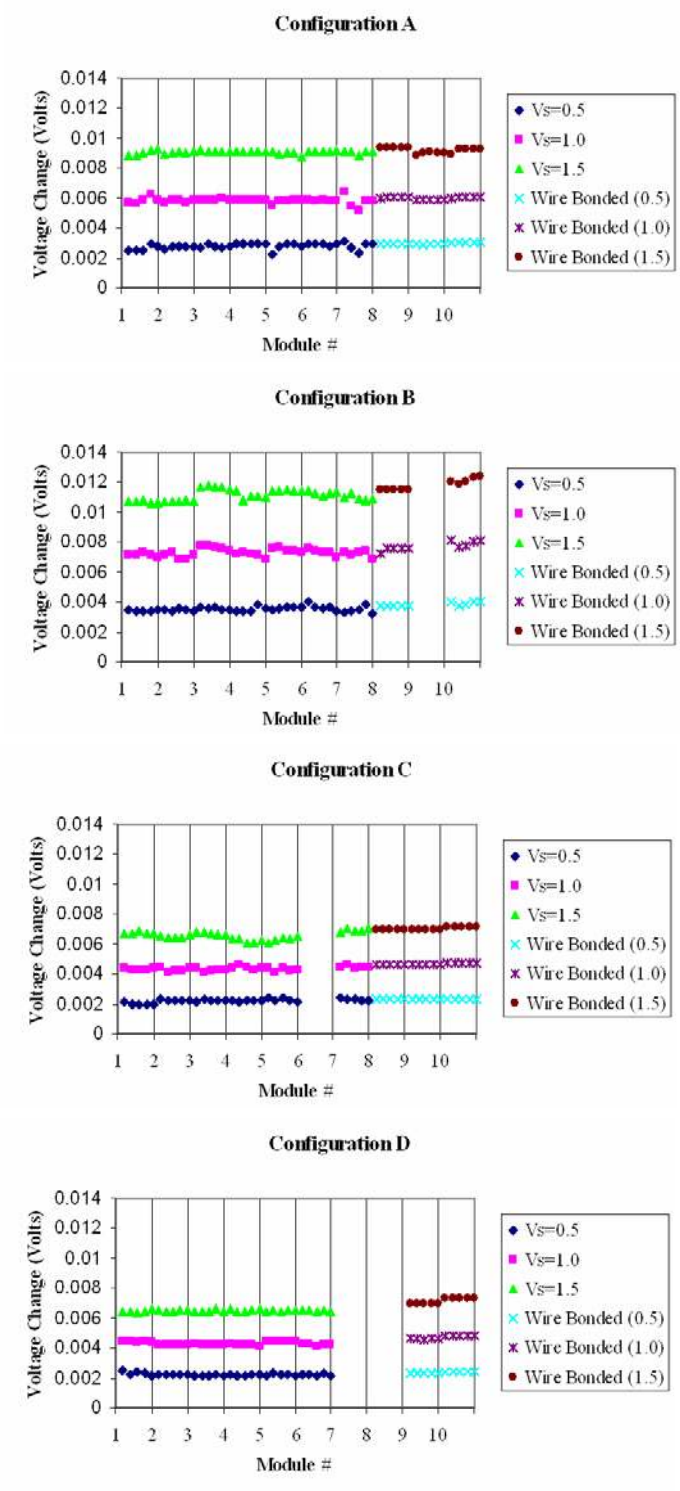

Figure 3.11: Experimental results for each configuration at three excitation voltages.

3.7 Conclusions

Resistance changes of a micro bistable mechanism as it toggles positions can be made to be detectable and repeatable. A 1.5 volt excitation voltage produced up to an 11.3 mV difference between the output voltage at each of the two stable positions. Ensuring that adequate compressive stresses are in the mechanism in its second stable state is one method of ensuring a measurable change between positions. This phenomenon can be modeled using finite element analysis, and the resulting trends may be used to enhance device design.

By using the mechanism as a sensing element in a Wheatstone bridge, on-chip sensing can be integrated into the system. Low power is needed to sense the state of the mechanism (2.8 mW for a 0.5 volt input), and the bridge configuration provides convenient, repeatable results. Time-varying factors and temperature dependencies are also eliminated by the use of the Wheatstone bridge.

A significant advantage of using piezoresistive properties rather than electrical contacts to detect state is that the reliability problems associated with electrical contacts can be eliminated, because the completion of an electrical circuit is no longer needed to determine the device position. Device design is thus simplified because no consideration must be taken for contact positioning, and device reliability is dramatically increased by eliminating the dependence on problematic micro contacts.

Possible applications for the bistable mechanism with piezoresistive position sensing include nonvolatile memory and high-acceleration sensing arrays. Bistable mechanisms are well-suited for nonvolatile memory applications, because they remain in position without any input power. Acceleration thresholds can be calculated using the mechanism switching force and the mass of the central shuttle. An array of mechanisms can be designed with varying acceleration thresholds. This array can then be queried following an impact to determine the magnitude of the experienced acceleration. Piezoresistivity may also be used to measure the dynamic response of a device by taking measurements as the device toggles.

CHAPTER 4 APPLICATIONS

4.1 Shock Sensor Array

The force required to flip a bistable mechanism can be reached by the interaction of an acceleration on the mass of the central shuttle of the mechanism. An array of bistable mechanisms with piezoresistive position sensing can be designed to determine the magnitude of shock loads. Changes in the mass of the mechanism's central shuttle alter the acceleration under which each switch will change positions. By determining which switches have flipped, the magnitude of the acceleration can be assessed. For example, if the 55 g (1 g= 9.81 m/s^2) switch flipped, but the 60g switch did not, the array experienced a load somewhere between these accelerations. An advantage of MEMS technology is the size of the mechanisms. A large number of mechanisms can be manufactured in a very small area, enabling the production of an array with very precise sensing capabilities.

Introduction

Package shock sensing is a promising market for the application of this technology. Over six billion packages are shipped each year by the three main shipping companies (UPS, FedEx, and DHL). Use of the package shock sensor on even a small percentage of shipped packages would utilize the savings received by the economies of scale experienced with MEMS manufacturing processes [35]. The package shock sensor could be used to prevent insurance fraud claiming damaged goods, to gather internal shipping route information, or as a perceived benefit by allowing the customer to track the shock level of their package while in-transit.

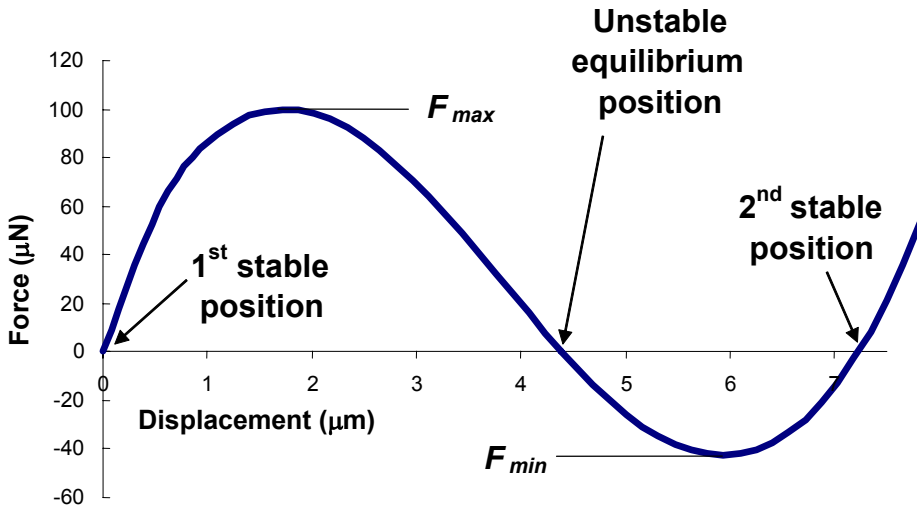

Figure 4.1: Typical force vs. displacement curve of a bistable mechanism.

The shock sensor could also be integrated into laptops to prevent warranty fraud. The repair company could detect if the error is due to component failure or user mishandling (e.g. dropping the computer).

Modeling

A typical force versus displacement curve of a bistable mechanism is shown in Figure 4.1, where F_{max} is the force required to actuate the mechanism from the first stable position to the second stable position, and F_{min} is the required force to return the mechanism to its original position. Changes in mechanism geometry result in the movement of the equilibrium positions and the magnitude of the forces required to switch between positions.

Commercially available shock sensors can be purchased with actuating accelerations between 5 and 200 g's. In order to produce a sensing array within this acceleration range, switching forces must be small (i.e. 5 μN or less), and the mass upon which the acceleration acts must be relatively large.

Two alternatives exist in the design of the acceleration-sensing bistable mechanisms with respect to the direction of actuation. The switching force at which the acceleration changes the mechanism's position, or critical force, could be either F_{max} or F_{min}. The use of F_{max} as the critical force presents some challenges. Conservation of energy dictates that the magnitude of F_{min} will always be less than F_{max}, due to the fact that the energy output from a system cannot exceed the energy input into the system. Thus, a latching mechanism must be used to hold the mechanism in the second stable position in order to prevent the mechanism from recoiling under lower accelerations.

The use of F_{min} as the critical force displays obvious advantages. In this configuration, the critical force can be small with the return force remaining relatively large. This eliminates the need for a latch, because the acceleration to return the switch to its second position is orders of magnitude larger than the critical acceleration. An additional manufacturing step is required to toggle the bistable mechanisms into their second stable or "cocked" positions. This initial positioning can be accomplished by the use of thermal in-plane microactuators (TIM) [36].

Due to the complexities of bistable mechanism design, a 2-D quarter-model finite element analysis (FEA) optimization was required to find a design with the appropriate switching forces. The optimization was performed using MatLab, with the FEA analyses executed in ANSYS. Target values were set for the switching forces and stress levels, and initial values for geometric dimensions were input. MatLab incrementally changed the geometric dimensions and executed ANSYS analyses until a mechanism was found with the desired characteristics.

Small variations in manufacturing processes and material properties can dramatically change the behavior of MEMS devices. Wittwer et al. [13] published methods for robust design using uncertainty analysis. Utilizing these methods, an optimization was executed including uncertainty analysis to design a mechanism with a critical force that is robust to common sources of variation associated with MEMS. The results of the uncertainty optimization are shown in Figure 4.2.

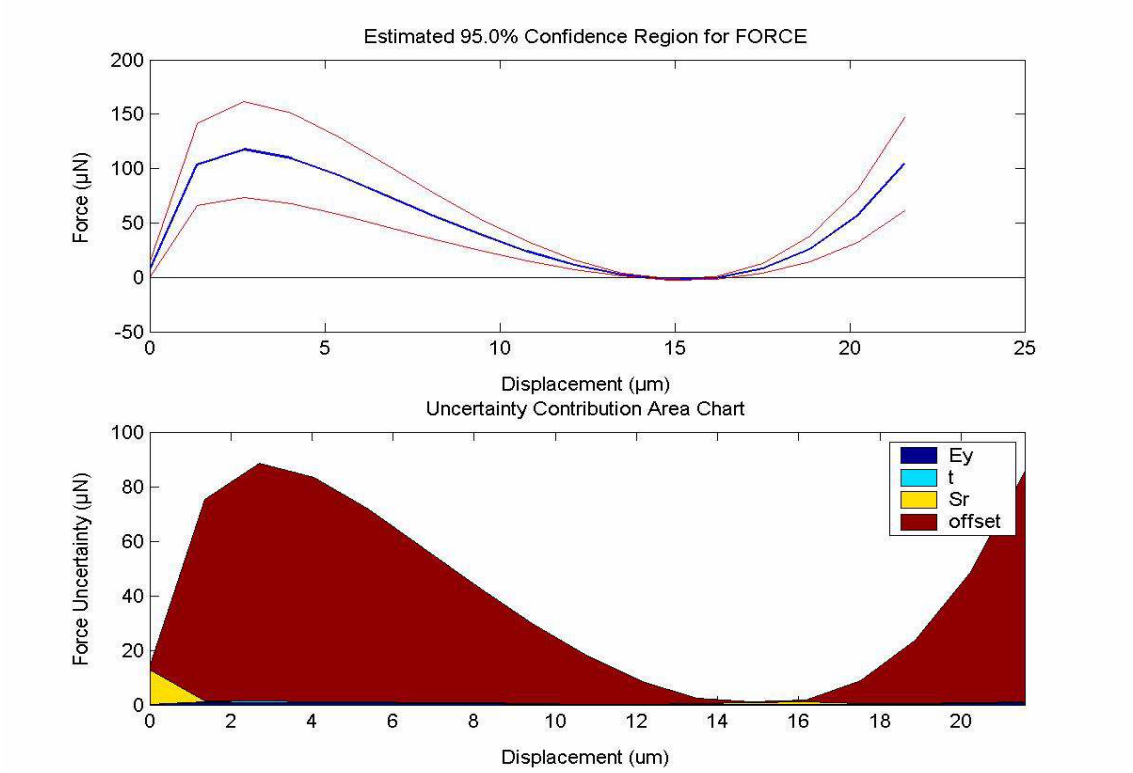

Figure 4.2: Results of uncertainty optimization for robust design.

The 95% confidence region shows the possible variation in the force throughout the mechanism's displacement. This variation is minimized in the area of the critical force. Large variation is present in areas along the curve, but it is irrelevant in this application. It can also be seen that the mechanism is bistable with 95% confidence since both error bands recede below the zero-line.

The main sources of variation can be seen in the uncertainty contribution area chart. The offset, or over-etch, was found to be the largest source of variation for this mechanism. Offset results from excess material being etched away during manufacturing, causing some dimensions to be produced smaller than they were originally designed. Other sources of variation are Young's modulus (E_y), out-of-plane thickness (t), and residual stress (S_r).

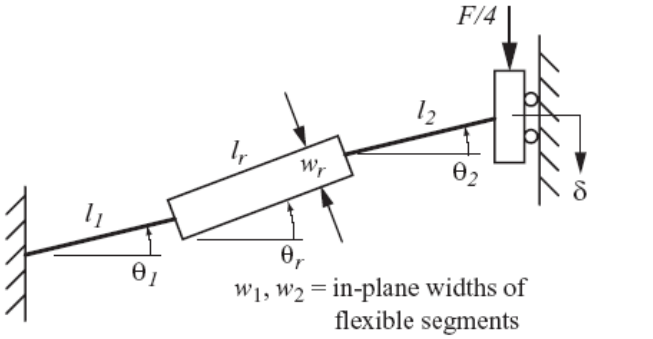

Figure 4.3: Design parameter description of the quarter-model of a fully compliant bistable mechanism [13].

The uncertainty optimization facilitated the design of a fully compliant bistable mechanism with a large switching force in the first direction, a small return force, and low force variation in the critical region. Insensitive to manufacturing and material variation, this mechanism is a robust, reliable design.

Designs

The design parameters for the fully compliant bistable micromechanism are shown in Figure 4.3. Values and design variables for the optimized acceleration sensing bistable mechanism are shown in Table 4.1 . The values represent dimensions as drawn for manufacturing using the SUMMiT IV process (an additional 0.2 μm will be removed from the three width dimensions due to over-etch).

Table 4.1: Design variables and optimized values.

Variable	Value
l_1 (μm)	40.01
w_1 (μm)	1.48
θ_1 (deg.)	9.37
l_r (μm)	29.13

Table 4.1: Design variables and optimized values.

Variable	Value
w_r (μm)	6.36
θ_r (deg.)	1.79
l_2 (μm)	40.01
w_2 (μm)	1.36
θ_2 (deg.)	10.0

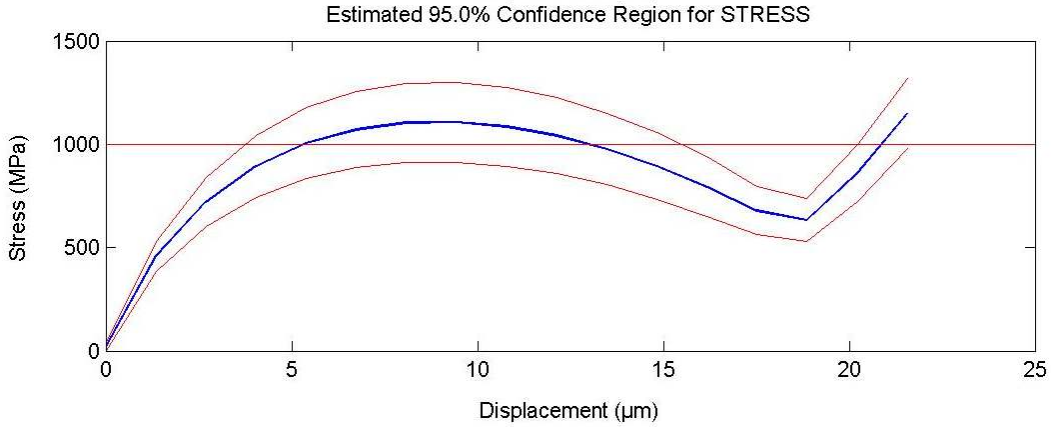

Figure 4.4: Maximum stress for optimized bistable micromechanism from uncertainty analysis.

The critical force, F_{min}, for this optimal design is predicted to be -2.188 μN, with a standard deviation of 0.328 μN. F_{max} is shown to be 117.78 μN, giving a switching ratio (F_{max}/F_{min}) of 54:1. The stress levels and distribution are also very conducive to piezoresistive sensing. The maximum stress level exceeds the conservative limit of 1000 MPa (Figure 4.4), but is below the maximum allowable stress for the polysilicon (approximately 1500 MPa). The stress is evenly distributed throughout the thin segments of the mechanism yielding a high average stress (Figure 4.5), which is also a desirable characteristic for piezoresistive sensing.

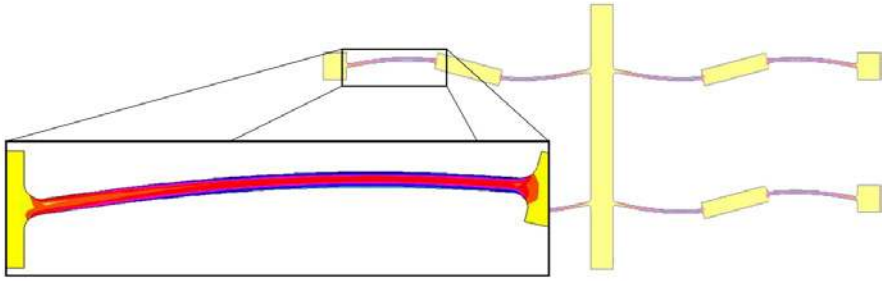

Figure 4.5: Finite element analysis stress distribution results in thin segments.

This optimized layout was modeled using the finite element model for configuration D as described in chapter three. Curves representing the voltage change as the mechanism toggles are seen in Figure 4.6 (the force-displacement plot is shown on the secondary axis for position reference). The device described in chapter three of this work necessitated a stop to hold the mechanism in a stressed state, due to the position of the voltage curve roots. The force-optimized design does not need a stop in the second stable position, because the zeroes of the voltage change curves are not located near the second stable equilibrium position. The voltage change with this design is predicted to be larger than the one seen in chapter three.

All switches in the acceleration sensing array use the same optimized bistable design. A variety of accelerations can be sensed by holding the force constant and adjusting the amount of mass on the central shuttle. This is accomplished by altering the area of the central shuttle. The relationship between actuating acceleration and shuttle area is shown in Figure 4.7. Along this curve the shuttle height (out-of-plane thickness) is held constant at 9 μm, utilizing all polysilicon layers of the SUMMiT IV manufacturing process.

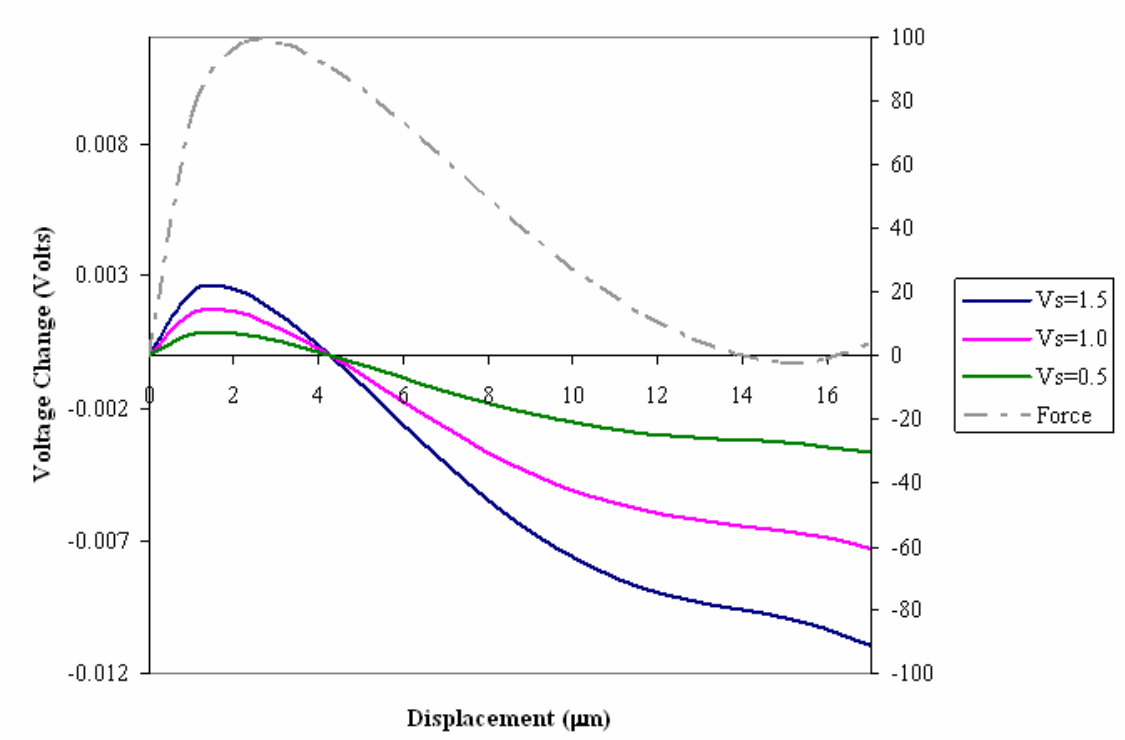

Figure 4.6: Voltage change curves of acceleration-sensing bistable mechanism.

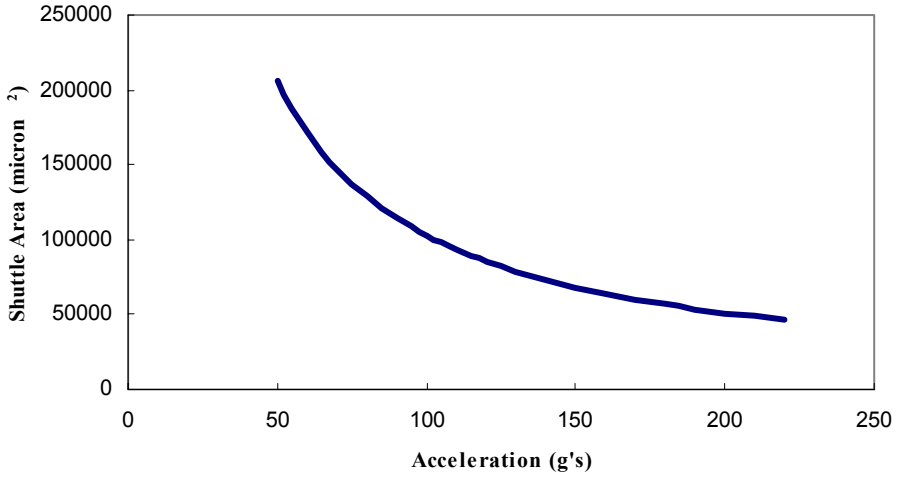

Figure 4.7: Relationship between actuating acceleration and shuttle area.

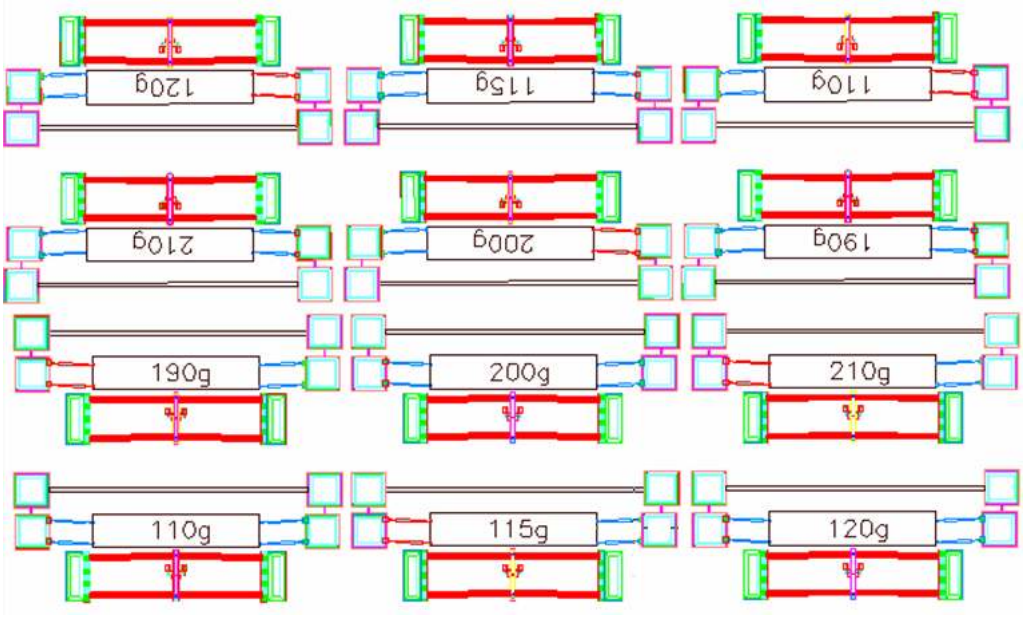

Figure 4.8: Example array demonstrating sensing capabilities along one axis.

Layout

The switches in the sensing array can be arranged to produce uni- or bi-directional acceleration sensing microchips. The number of sensing axes depends on the desired applications and cost trade-offs. Package shock sensing could achieve detection along three axes by utilizing three uni-directional arrays (one aligned along each axis) or two bi-direction arrays (one on two different, perpendicular axes). Each array requires two sets of bistable mechanisms for each axis of detection, one facing each direction along an axis. An example uni-directional array can be seen in Figure 4.8.

4.2 Nonvolatile Memory

Another promising application of bistable micromechanisms with piezoresistive sensing capabilities is in nonvolatile memory. Hälg [32] investigated the use of a thin bridge which elastically deformed between two positions to achieve bistability. The bridge position was switched using electrostatic forces, and the position of the bridge was detected by sensing the corresponding capacitance.

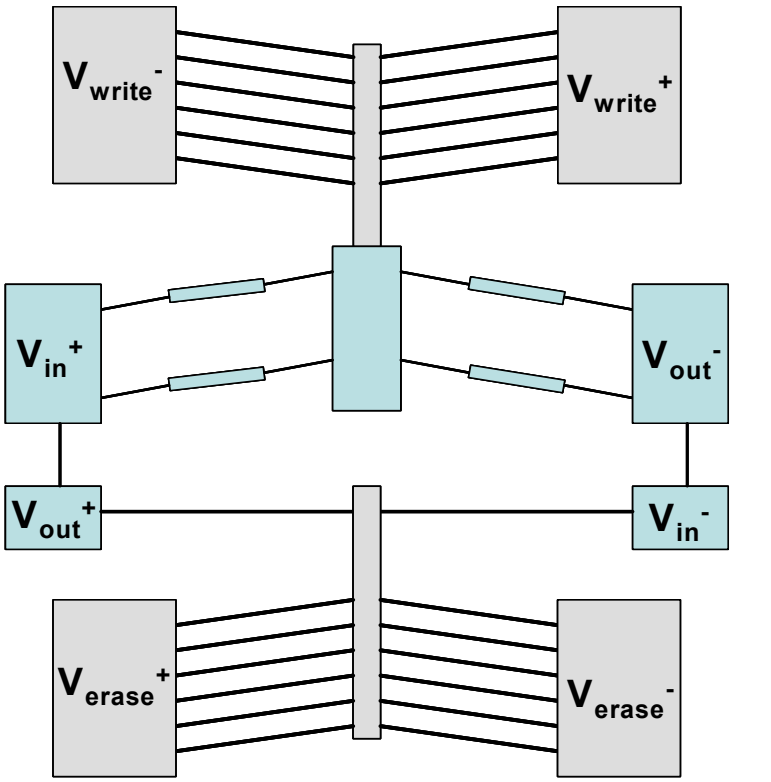

Figure 4.9: Bistable mechanism with thermal actuators.

Bistable mechanisms are ideally suited for use in nonvolatile memory due to their inherent property of staying in position for an unlimited time without the need of external energy. Thus, if power to an electronic device fails, the bistable mechanisms will preserve vital information by remaining in their last written positions. Each position of the bistable mechanism is conventionally assigned either the erased state ("0") or written state ("1") [37].

Thermal in-plane microactuators (TIM) [36] are used to actuate the bistable mechanism back and forth between its two stable equilibrium positions. One bit of nonvolatile memory is shown in Figure 4.9. Information is stored in this bit by applying a voltage across the top TIM, or it is erased by energizing the lower TIM. Interference between the TIM and sensing beams is avoided by creating the devices in different layers. The piezoresistive sensing beams of the bistable mechanism are manufactured in the first layer, poly0.

The TIM uses the top two layers, poly3 and poly4, thus avoiding the sensing beams both mechanically and electrically. The memory can be read by reading the voltage off the Wheatstone bridge configuration and interpreting the results to reveal the position of the bistable mechanism.

The memory can be written or erased as quickly as the TIM can actuate the mechanism. TIMs have a response time of 500 μs [28] which corresponds to the device's write/erase time. Competing technology, such as flash electrically erasable programmable read-only memory (Flash EEPROM), has write times of 10 μs/byte [38]. Design for uncertainty [13] produces reliable devices with predictable behavior. Bistable mechanisms have been cycled over 2 million times without failure [15], while thermal actuators have shown long life cycles pending the input current does not change material properties [39]. This technology also has the advantages of low power consumption, and immunity to electro-magnetic fields. Disadvantages of this technology include the configuration's large size and relatively slower write times than conventional flash memory. The size could potentially be reduced by designing bistable mechanisms and thermal actuators specific to this application. The SUMMiT process also allows the stacking of devices which could reduce the area of the device.

CHAPTER 5 CONCLUSIONS AND RECOMMENDATIONS

5.1 Conclusions

Resistance changes of a micro bistable mechanism as it toggles positions are detectable and repeatable. A 1.5 V excitation voltage produced up to a 11.27 mV difference between the output voltage at each of the two stable positions. This phenomenon can be modeled in finite element analysis, and the resulting trends can be used to improve device design and predict when the use of stops is necessary in the second stable equilibrium position (i.e. the device in chapter 3 necessitates a stop, but the force-optimized mechanism in chapter 4 performs better without a stop).

On-chip sensing is integrated into the actual device as the mechanism is used as a sensing element in a Wheatstone bridge. Low power is needed to sense the state of the mechanism, and the bridge configuration provides convenient, repeatable results. Time-varying factors are also eliminated by the use of the Wheatstone bridge. Electrical contacts can be eliminated, because the completion of an electrical circuit is no longer needed to determine the device position. Device design is thus simplified because no consideration must be taken for contact positioning. Piezoresistivity may also be used to measure the dynamic response of a device by taking measurements as the device toggles.

Possible applications for the bistable mechanism with piezoresistive position sensing include nonvolatile memory and high-acceleration sensing arrays. A bistable mechanism was designed for use in a shock sensing array. The switching force in the sensitive direction is predicted to be 2.188 μN, with a standard deviation of 0.328 μN. The magnitude of the actuating acceleration can vary depending on the size of the shuttle mass.

5.2 Recommendations

Modeling accuracy could be improved by determining the piezoresistive coefficients for the process-specific polysilicon. Further applications should be explored, along with the use of the device in a marketable product. More modeling and testing should be done to determine the effects of different stress types (i.e. bending, axial, shear) on the piezoresistive effect. A sensitivity analysis would help better understand the effects of small variations in geometric dimensions, piezoresistive coefficients, and material properties. Uncertainty analysis optimizations could be used to design devices with very large output signals while minimizing variation in this signal.

REFERENCES

[1] Howell, L.L., 2001, *Compliant Mechanisms*, John Wiley & Sons, New York.

[2] Madou, M., 1997, *Fundamentals of Microfabrication*, CRC Press, Boca Raton, FL.

[3] Maluf, N., 2000, *An Introduction to Microelectromechanical Systems Engineering*, Artech House, Norwood, MA.

[4] Jensen, B.D., 1998, Identification of Macro- and Micro- Compliant Mechanism Configurations Resulting in Bistable Behavior, M.S. Thesis, Brigham Young University, Provo, UT.

[5] Parkinson, M.B., Jensen, B.D., and Roach, G.M., 2000, "Optimization-Based Design of a Fully-Compliant Bistable Micromechanism," *2000 ASME Design Engineering Technical Conferences and Computer and Information in Engineering Conference*, Sept. 10-13, 2000, Baltimore, Maryland.

[6] Foulds, I., Trinh, M., Hu, S., Liao, S., Johnstone, R., Parameswaran, M., 2002, "A Surface Micromachined Bistable Switch," *IEEE CCECE2002*, Vol. 1, pp. 465-469.

[7] Wagner, B., Quenzer, H.J., Hoerschelmann, S., Lisec, T., Juerss, M., 1996, "Bistable Microvalve with Pneumatically Coupled Membranes," *9th International IEEE Conference*, pp. 384-388.

[8] Qiu, J., Lang, J.H., Slocum, A. H., Strumpler, R., 2003, “A High-Current Electrothermal Bistable MEMS Relay,” *16th Internation IEEE Conference on Micro Electro Mechanical Systems (MEMS)*, pp. 64-67.

[9] Opdahl, P.G., 1996, Modeling and Analysis of Compliant Bi-Stable Mechanisms Using the Pseudo-Rigid-Body Model, M.S. Thesis, Brigham Young University, Provo, UT.

[10] Opdahl, P. G., Jensen, B.D., and Howell, L.L., 1998, “An Investigation into Compliant Bistable Mechanisms,” *Proceedings of the 1998 ASME Design Engineering Technical Conferences*, DETC09/DAC-3763.

[11] Jensen, B.D., Howell, L.L., Salmon, L.G., 1998, “Design of Two-Link, In-Plane, Bistable Compliant Micro-Mechanisms”, *Proceeding of the 1998 ASME Design Engineering Technical Conferences*, DETC98/MECH-5837.

[12] Baker, M.S., Lyon, S.M., and Howell, L.L., 2000, "A Linear Displacement Bistable Micromechanism,” *Proceedings of the 2000 ASME Design Engineering Technical Conferences*, DETC2000/MECH-14117, pp. 1-7.

[13] Wittwer, J.W., Baker, M.S., Howell, L.L., 2005, “Robust Design and Model Validation of Nonlinear Compliant Micromechanisms,” *Submitted to: Journal of Microelectromechanical Systems*, March 1, 2005.

[14] Qui, J., Lang, J.H., Slocum, A.H., 2001, “A Centrally-Clamped Parallel-Beam Bistable MEMS Mechanism,” *14th International IEEE Conference*, pp. 353-356.

[15] Masters, N.D., Howell, L.L., 2003, “A Self-Retracting Fully Compliant Micromechanism,” *Journal of Microelectromechanical Systems*, Vol. 12, No. 3, pp. 273-280.

[16] Wittwer, J.W., Wait, S.M., Howell, L.L., Cherry, M.S., 2002, “Predicting the performance of a bistable micro mechanism using design-stage uncertainty analysis,” *ASME*, Micro-Electromechanical Systems Division Publication (MEMS), pp. 127-134.

[17] Smith, C.S., 1954, “Piezoresistance Effect in Germanium and Silicon,” *Physical Review*, 94,pp. 42-49.

[18] Elgamel, H.E., 1995, “Closed-form expressions for the relationships between stress, diaphragm deflection, and resistance change with pressure in silicon piezoresistive pressure sensors,” *Sensors and Actuators*, 50, pp. 17-22.

[19] Eaton, W.P., 1997, “Surface Micromachined Pressure Sensors,” Ph.D. Dissertation, University of New Mexico, Albuquerque, NM.

[20] French, P.J., Evans, A.G.R., 1989, “Piezoresistance in Polysilicon and its Applications to Strain Gauges,” *Solid State Electronics*, Vol. 32, No. 1, pp. 1-10.

[21] Wymyslowski, A., Santo-Zarnki, M., Friedel, K., Belavic, D., 2004, "Numerical simulation and Experimental Verification of the Piezoresistivity Phenomenon for the Printed Thick-Film Piezoresistors," *Proceedings of the 5th International Conference on Thermal and Mechanical Simulation and Experiments in Microelectronics and Microsystems*, pp. 359-366.

[22] French, P.J., Evans, A.G.R., 1985, "Polycrystalline silicon strain sensors," *Sensors and Actuators*, 8, pp. 219-225.

[23] French, P.J., Evans, A.G.R., 1986, "Polycrystalline silicon as a strain gauge material," *Journal of Physics E: Scientific Instruments*, 19, pp. 1055-1058.

[24] Burns, D., 1988, "Micromechanics of Integrated Sensors and the Planar Processed Pressure Transducer," Ph.D. dissertation, University of Wisconsin-Madison.

[25] Eaton, W.P., Smith, J.H., "Planar Surface-Micromachined Pressure Sensor with a Sub-Surface, Embedded Reference Pressure Cavity," *Proceeding of the SPIE*, Vol. 2882.

[26] Schellin, R., Hess, G., 1992, "Silicon subminiature microphone based on piezoresistive polysilicon strain gauges," *Sensors and Actuators*, v. 32, n. 1-3, pp. 555-559.

[27] Liang, Y., Kenny, T., 1998, "Mechanical optimization of a dual-axis piezoresistive force sensor," *ASME*, DSC Division, MEMS v. 66, pp. 389-394.

[28] Messenger, R.K., 2004, Modeling and Control of Surface Micromachined Thermal Actuators, M.S. Thesis, Brigham Young University, Provo, UT.

[29] Messenger, R.K., McLain, T.W., Howell, L.L., 2004, "Feedback Control of a Thermomechanical Inplane Microactuator Using PiezoResistive Displacement Sensing", *Proceeding of 2004 ASME International Mechanical Engineering Congress*, IMECE2004-59810.

[30] Gad-el-Hak, M., 2001, *The MEMS Handbook*, CRC Press, Boca Raton, FL.

[31] Gridchin, V.A., Lubimsky, V.M., 2003, "Phenomonological Model of the Piezoresistive Effect in Polysilicon Films," *Russian Microelectronics*, Vol. 32, No. 4, pp. 205-213.

[32] Hälg, B., 1990, "On a Micro-Electro-Mechanical Nonvolatile Memory Cell," *Proceedings of IEEE Micro-Electro-Mechanical Systems*, An Investigation on Micro Structures, Sensors, Actuators, Machines and Robots, pp. 172-176.

[33] Koester, D.A., Mahadevan, R., Hardy, B., Markus, K.W., 2001, *MUMPs Design Handbook*, Research Triangle Park, N.C.: Cronos Integrated Microsystems.

[34] Lott, C.D., McClain, T.W., Harb, J.N., Howell, L.L., 2001, "Thermal Modeling of a Surface-Micromachined Linear Thermal Actuator", *Modeling and Simulation of Microsystems*, pp. 370-373.

[35] Tadigadapa, S., Najifi, N., "Developments in microelectromechanical systems (MEMS): A manufacturing perspective," *Journal of Manufacturing Science and Engineering*, Vol. 125, No. 4, pp. 816-823.

[36] Cragun, R., 1998, "Constrained thermal expansion micro-actuator," *ASME*, Dynamic Systems and Control Division (Publication) DSC, 66, Micro-Electro-Mechanical Systems (MEMS), p. 365-371.

[37] Brown, W.D., Brewer, J.E., 1998, *Nonvolatile Semiconductor Memory Technology: A Comprehensive Guide to Understanding and Using NVSM Devices*. IEEE Press, New York.

[38] Hu, C., 1991, *Nonvolatile Semiconductor Memories: Technologies, Design, and Applications*. IEEE Press, New York, p. 6.

[39] Cragun, R., 1999, Thermal Actuators for Microelectromechanical Systems (MEMS), M.S. Thesis, Brigham Young University, Provo, UT.

Appendix

APPENDIX A

Configuration A

```
!=============================================================
! Created by Jeff Anderson, 20 Jun 05
!  This batch file uses 8-Node Coupled-Field Solid elements to analyze the piezoresistivity
          of a Fully
!  Compliant Bistable Mechanism.
!  Config A- see thesis for configuration description
!
!=============================================================
/TITLE,Analysis of a Fully Compliant Bistable Mechanism
/CLEAR,NOSTART
/PREP7
PI=acos(-1)
!=============================================================
!              INPUT PARAMETERS
!=============================================================
t = 4.75
L1 = 21.6
h1 = 1.5
theta1 = 0.122454045649174
```

```
L2 = 21.6
h2 = 1.45
theta2 = 0.0355872634481644
Lr = 80
hr = 6
thetar = 0.0378212848907171
swidth=9.8
sheight=83.8

Ey = 164000
Pr = 0.23
NLegs=2
dY = -10
rho = 11.7e-8  !Resistivity (n-type Si)
p11=-102.2e-5
p12=53.4e-5
p44=-13.6e-5

Vs=1.0
Vg=0
/NOPR

ET,1,PLANE223,101

R,1,t
MP,EX,1,Ey     !*** Youngs Modulus ***
MP,PRXY,1,Pr   !*** Poisson's Ratio ***
MP,RSVX,1,rho

TB,PZRS,1
TBDATA,1,P11,P12,P12
```

```
TBDATA,7,P12,P11,P12
TBDATA,13,P12,P12,P11
TBDATA,22,P44

Nonlinear = 1
Steps = 16
!============================================================
!            RELATIONAL PARAMETERS
!============================================================

Lx=L1*cos(theta1)+Lr*cos(thetar)+L2*cos(theta2)
Ly=L1*sin(theta1)+Lr*sin(thetar)+L2*sin(theta2)

!============================================================
!            MODEL SETUP
!============================================================
K,3,0,0,0
K,4,0,h1/(2*sin(PI/2-theta1)),0
K,5,0,-h1/(2*sin(PI/2-theta1)),0
K,8,L1*cos(theta1)-h1/2*sin(theta1),L1*sin(theta1)+h1/2*cos(theta1),0
K,9,L1*cos(theta1),L1*sin(theta1),0
K,10,L1*cos(theta1)+h1/2*sin(theta1),L1*sin(theta1)-h1/2*cos(theta1),0
K,11,L1*cos(theta1)-hr/2*sin(thetar),L1*sin(theta1)+hr/2*cos(thetar),0
K,12,L1*cos(theta1)+Lr*cos(thetar)-hr/2*sin(thetar),L1*sin(theta1)+Lr*sin(thetar)+hr/
        2*cos(thetar),0
K,13,L1*cos(theta1)+Lr*cos(thetar)-h2/2*sin(theta2),L1*sin(theta1)+Lr*sin(thetar)+h2/
        2*cos(theta2),0
K,14,L1*cos(theta1)+Lr*cos(thetar),L1*sin(theta1)+Lr*sin(thetar),0
K,15,L1*cos(theta1)+Lr*cos(thetar)+h2/2*sin(theta2),L1*sin(theta1)+Lr*sin(thetar)-h2/
        2*cos(theta2),0
```

```
K,16,L1*cos(theta1)+Lr*cos(thetar)+hr/2*sin(thetar),L1*sin(theta1)+Lr*sin(thetar)-hr/
      2*cos(thetar),0
K,17,L1*cos(theta1)+hr/2*sin(thetar),L1*sin(theta1)-hr/2*cos(thetar),0
K,18,Lx,Ly,0
K,19,Lx,Ly+h2/(2*sin(PI/2-theta2)),0
K,20,Lx,Ly+sheight/Nlegs/2,0
K,21,Lx+swidth/2,Ly+sheight/Nlegs/2,0
K,22,Lx+swidth/2,Ly-sheight/Nlegs/2,0
K,23,Lx,Ly-sheight/Nlegs/2,0
K,24,Lx,Ly-h2/(2*sin(PI/2-theta2)),0

L,4,8
L,8,11
L,11,12
L,12,13
L,13,19
L,19,20
L,20,21
L,21,22
L,22,23
L,23,24
L,24,15
L,15,16
L,16,17
L,17,10
L,10,5
L,5,4
LFILLT,1,2,h1
LFILLT,14,15,h1
LFILLT,4,5,h2
LFILLT,5,6,h2
```

```
LFILLT,10,11,h2
LFILLT,11,12,h2

AL,ALL
AGEN,Nlegs,1,1,1,0,-sheight/Nlegs,0,0,0,0
ARSYM,X,ALL,0,0,0
AGEN,2,Nlegs+1,2*Nlegs,1,Lx+swidth/2,0,0,0,0,1
AGEN,2,Nlegs+1,2*Nlegs,1,Lx+swidth/2,0,0,0,0,1
AADD,ALL

ARSYM,Y,ALL,0,0,0
AGEN,2,1,1,1,0,-sheight-2*Lx,0,0,0,1
ARSYM,X,5,0,0,0
AGEN,2,2,2,1,0,-Lx,0,0,0,1
ARSYM,X,5,0,0,0
AGEN,2,3,3,1,4*Lx,-Lx,0,0,0,1

!*** MESH MECHANISMS ***
real,1
type,1
mat,1

AESIZE,ALL,h1/2
AMESH,ALL
LREFINE,1,1,1,2,2,CLEAN,ON
LREFINE,23,1,1,2,2,CLEAN,ON
LREFINE,5,1,1,2,2,CLEAN,ON
LREFINE,29,1,1,2,2,CLEAN,ON
LREFINE,51,1,1,2,2,CLEAN,ON
LREFINE,73,1,1,2,2,CLEAN,ON
LREFINE,45,1,1,2,2,CLEAN,ON
```

```
LREFINE,67,1,1,2,2,CLEAN,ON

!*** Get Node Number at KeyPoint 21 ***
ksel,s,kp,,21
nslk,s
*get,nkp1,node,0,num,max
nsel,all
ksel,all

!============ Electrical Boundary Contraints  =============

LSEL,S,LINE,,16        !Define supply voltage contact
LSEL,A,LINE,,44
LSEL,A,LINE,,198
LSEL,A,LINE,,179
NSLL,S,1
CP,1,VOLT,ALL
*GET,ns,NODE,0,NUM,MIN
D,NS,VOLT,Vs

LSEL,S,LINE,,278       !Define ground contact
LSEL,A,LINE,,259
LSEL,A,LINE,,158
LSEL,A,LINE,,139
NSLL,S,1
CP,2,VOLT,ALL
*GET,ng,NODE,0,NUM,MIN
D,NG,VOLT,0

LSEL,S,LINE,,219        !Define first output contact
LSEL,A,LINE,,238
```

```
LSEL,A,LINE,,99
LSEL,A,LINE,,118
NSLL,S,1
CP,3,VOLT,ALL
*GET,no1,NODE,00,NUM,MIN

LSEL,S,LINE,,66        !Define second output contact
LSEL,A,LINE,,88
LSEL,A,LINE,,299
LSEL,A,LINE,,318
NSLL,S,1
CP,4,VOLT,ALL
*GET,no2,NODE,0,NUM,MIN
NSEL,ALL
LSEL,ALL

!========== Structural Boundary Constraints ==========

DL,16,,UX,0
DL,16,,UY,0
DL,44,,UX,0
DL,44,,UY,0
DL,66,,UX,0
DL,66,,UY,0
DL,88,,UX,0
DL,88,,UY,0

DK,21,UY,-dY
FINISH

!=====================================================
```

```
!              SOLUTION STEPS
!=============================================================
/SOLU

NLGEOM,1       !***Nonlinear Analysis****
ANTYPE,0       !***Static Analysis Type***


!============ VERTICAL DISPLACEMENT =============
*DO,mm,1,Steps+1,1
  DK,21, ,(mm-1)*dY/Steps, , , ,UY, , , , ,
  lswrite,mm
*ENDDO

lssolve,1,Steps+1

FINISH

/POST1


!=========== RETRIEVE IMPORTANT DATA ===

*DIM,Smax,TABLE,Steps+1
*DIM,Ydis,TABLE,Steps+1
*DIM,Force,TABLE,Steps+1
*DIM,VoltO1,TABLE,Steps+1
*DIM,VoltO2,TABLE,Steps+1
*DO,n,1,Steps+1,1
Set,n
```

```
ETABLE,svonm,S,EQV

ESORT,ETAB,svonm,0,1
*GET,Smax(n),SORT,0,MAX

*GET,Ydis(n),NODE,nkp1,U,Y

*GET,Force(n),NODE,nkp1,RF,FY

*GET,VoltO1(n),NODE,no1,VOLT
*GET,VoltO2(n),NODE,no2,VOLT
*ENDDO

!Create Output File

/output,Configuration_A_results.txt
*VWRITE
YdisYforceSmaxVoltO1VoltO2
*VWRITE,Ydis(1),Force(1),Smax(1),VoltO1(1),VoltO2(1)
%15e %15e %15e %15e %15e
/output
FINISH
```

Configuration B

```
!=============================================================
!  Created by Jeff Anderson, 20 Jun 05
!  This batch file uses 8-Node Coupled-Field Solid elements to analyze the piezoresistivity
        of a Fully
!  Compliant Bistable Mechanism.
!  Config B- see thesis for configuration description
!
```

```
!=============================================================
/TITLE,Analysis of a Fully Compliant Bistable Mechanism
/CLEAR,NOSTART
/PREP7
PI=acos(-1)
!=============================================================
!              INPUT PARAMETERS
!=============================================================
t = 4.75
tr= 0.3
L1 = 21.6
h1 = 1.5
theta1 = 0.122454045649174
L2 = 21.6
h2 = 1.45
theta2 = 0.0355872634481644
Lr = 80
hr = 6
thetar = 0.0378212848907171
swidth=9.8
sheight=83.8

Wb= 9.367  !Width of the resistive beam
Lb= 26    !Length of the resistive beam

Ey = 164000
Pr = 0.23
NLegs=2
dY = -10
rho = 11.7e-8  !Resistivity (n-type Si)
p11=-102.2e-5
```

```
p12=53.4e-5
p44=-13.6e-5

Vs=1.5
Vg=0
/NOPR

ET,1,PLANE223,101

R,1,t
R,2,tr
MP,EX,1,Ey     !*** Youngs Modulus ***
MP,PRXY,1,Pr   !*** Poisson's Ratio ***
MP,RSVX,1,rho

TB,PZRS,1
TBDATA,1,P11,P12,P12
TBDATA,7,P12,P11,P12
TBDATA,13,P12,P12,P11
TBDATA,22,P44

Nonlinear = 1
Steps = 16
!=============================================================
!              RELATIONAL PARAMETERS
!=============================================================

Lx=L1*cos(theta1)+Lr*cos(thetar)+L2*cos(theta2)
Ly=L1*sin(theta1)+Lr*sin(thetar)+L2*sin(theta2)

!=============================================================
```

```
!              MODEL SETUP
!=========================================================
K,3,0,0,0
K,4,0,h1/(2*sin(PI/2-theta1)),0
K,5,0,-h1/(2*sin(PI/2-theta1)),0
K,8,L1*cos(theta1)-h1/2*sin(theta1),L1*sin(theta1)+h1/2*cos(theta1),0
K,9,L1*cos(theta1),L1*sin(theta1),0
K,10,L1*cos(theta1)+h1/2*sin(theta1),L1*sin(theta1)-h1/2*cos(theta1),0
K,11,L1*cos(theta1)-hr/2*sin(thetar),L1*sin(theta1)+hr/2*cos(thetar),0
K,12,L1*cos(theta1)+Lr*cos(thetar)-hr/2*sin(thetar),L1*sin(theta1)+Lr*sin(thetar)+hr/
        2*cos(thetar),0
K,13,L1*cos(theta1)+Lr*cos(thetar)-h2/2*sin(theta2),L1*sin(theta1)+Lr*sin(thetar)+h2/
        2*cos(theta2),0
K,14,L1*cos(theta1)+Lr*cos(thetar),L1*sin(theta1)+Lr*sin(thetar),0
K,15,L1*cos(theta1)+Lr*cos(thetar)+h2/2*sin(theta2),L1*sin(theta1)+Lr*sin(thetar)-h2/
        2*cos(theta2),0
K,16,L1*cos(theta1)+Lr*cos(thetar)+hr/2*sin(thetar),L1*sin(theta1)+Lr*sin(thetar)-hr/
        2*cos(thetar),0
K,17,L1*cos(theta1)+hr/2*sin(thetar),L1*sin(theta1)-hr/2*cos(thetar),0
K,18,Lx,Ly,0
K,19,Lx,Ly+h2/(2*sin(PI/2-theta2)),0
K,20,Lx,Ly+sheight/Nlegs/2,0
K,21,Lx+swidth/2,Ly+sheight/Nlegs/2,0
K,22,Lx+swidth/2,Ly-sheight/Nlegs/2,0
K,23,Lx,Ly-sheight/Nlegs/2,0
K,24,Lx,Ly-h2/(2*sin(PI/2-theta2)),0

L,4,8
L,8,11
L,11,12
L,12,13
```

```
L,13,19
L,19,20
L,20,21
L,21,22
L,22,23
L,23,24
L,24,15
L,15,16
L,16,17
L,17,10
L,10,5
L,5,4
LFILLT,1,2,h1
LFILLT,14,15,h1
LFILLT,4,5,h2
LFILLT,5,6,h2
LFILLT,10,11,h2
LFILLT,11,12,h2

AL,ALL
AGEN,Nlegs,1,1,1,0,-sheight/Nlegs,0,0,0,0
ARSYM,X,ALL,0,0,0
AGEN,2,Nlegs+1,2*Nlegs,1,Lx+swidth/2,0,0,0,0,1
AGEN,2,Nlegs+1,2*Nlegs,1,Lx+swidth/2,0,0,0,0,1
AADD,ALL

AGEN,2,5,5,1,0,-131,0,0,0,0      !Create second bistable mechanism

L,45,138!Connect the shuttles
L,89,140
AL,34,91,162,129,128,161
```

```
AADD,ALL



K,200,-5,-sheight/2,0    !Create 1st Beam Resistor
K,201,-5-Wb,-sheight/2,0
K,202,-5-Wb,-sheight/2-Lb,0
K,203,-5,-sheight/2-Lb,0
L,200,201
L,201,202
L,202,203
L,203,200
AL,34,129,128,91

K,204,2*Lx+swidth+5,-sheight/2,0
K,205,2*Lx+swidth+5+Wb,-sheight/2,0
K,206,2*Lx+swidth+5+Wb,-sheight/2-Lb,0
K,207,2*Lx+swidth+5,-sheight/2-Lb,0
L,204,205
L,205,206
L,206,207
L,207,204
AL,163,164,165,166

!*** MESH MECHANISM ***
real,1
type,1
mat,1

AESIZE,3,h1/3
```

```
AMESH,3

!*** MESH BEAM RESISTORS ***
real,2
type,1
mat,1

AESIZE,1,wb/3
AESIZE,2,wb/3
AMESH,1,2,1

!*** Get Node Number at KeyPoint 21 ***
ksel,s,kp,,21
nslk,s
*get,nkp1,node,0,num,max
nsel,all
ksel,all

!============ Electrical Boundary Contraints  =============

LSEL,S,LINE,,16        !Define supply voltage contact
LSEL,A,LINE,,44
LSEL,A,LINE,,34
NSLL,S,1
CP,1,VOLT,ALL
*GET,ns,NODE,0,NUM,MIN
D,NS,VOLT,Vs

LSEL,S,LINE,,165       !Define ground contact
LSEL,A,LINE,,139
LSEL,A,LINE,,158
```

```
NSLL,S,1
CP,2,VOLT,ALL
*GET,ng,NODE,0,NUM,MIN
D,NG,VOLT,0

LSEL,S,LINE,,128        !Define first output contact
LSEL,A,LINE,,118
LSEL,A,LINE,,99
NSLL,S,1
CP,3,VOLT,ALL
*GET,no1,NODE,00,NUM,MIN

LSEL,S,LINE,,66        !Define second output contact
LSEL,A,LINE,,88
LSEL,A,LINE,,163
NSLL,S,1
CP,4,VOLT,ALL
*GET,no2,NODE,0,NUM,MIN
NSEL,ALL
LSEL,ALL

!========== Structural Boundary Constraints ==========

DL,16,,UX,0
DL,16,,UY,0
DL,44,,UX,0
DL,44,,UY,0
DL,66,,UX,0
DL,66,,UY,0
DL,88,,UX,0
DL,88,,UY,0
```

```
DL,118,,UX,0
DL,118,,UY,0
DL,99,,UX,0
DL,99,,UY,0
DL,139,,UX,0
DL,139,,UY,0
DL,158,,UX,0
DL,158,,UY,0

DK,21,UY,-dY
FINISH

!=========================================================
!              SOLUTION STEPS
!=========================================================
/SOLU

NLGEOM,1       !***Nonlinear Analysis****
ANTYPE,0       !***Static Analysis Type***


!============ VERTICAL DISPLACEMENT ==============
*DO,mm,1,Steps+1,1
  DK,21, ,(mm-1)*dY/Steps, , , ,UY, , , , ,
  lswrite,mm
*ENDDO

lssolve,1,Steps+1

FINISH
```

```
/POST1

!========== RETRIEVE IMPORTANT DATA ===

*DIM,Smax,TABLE,Steps+1
*DIM,Ydis,TABLE,Steps+1
*DIM,Force,TABLE,Steps+1
*DIM,VoltO1,TABLE,Steps+1
*DIM,VoltO2,TABLE,Steps+1
*DO,n,1,Steps+1,1
Set,n

ETABLE,svonm,S,EQV

ESORT,ETAB,svonm,0,1
*GET,Smax(n),SORT,0,MAX

*GET,Ydis(n),NODE,nkp1,U,Y

*GET,Force(n),NODE,nkp1,RF,FY

*GET,VoltO1(n),NODE,no1,VOLT
*GET,VoltO2(n),NODE,no2,VOLT
*ENDDO

!Create Output File

/output,Configuration_B_results.txt
*VWRITE
YdisYforceSmaxVoltO1VoltO2
*VWRITE,Ydis(1),Force(1),Smax(1),VoltO1(1),VoltO2(1)
```

%15e %15e %15e %15e %15e

/output

FINISH

Configuration C

```
!=============================================================
!  Created by Jeff Anderson, 20 Jun 05
!  This batch file uses 8-Node Coupled-Field Solid elements to analyze the piezoresistivity
        of a Fully
!  Compliant Bistable Mechanism.
!  Config C- see thesis for configuration description
!
!=============================================================
/TITLE,Analysis of a Fully Compliant Bistable Mechanism
/CLEAR,NOSTART
/PREP7
PI=acos(-1)
!=============================================================
!             INPUT PARAMETERS
!=============================================================
t = 4.75
tvr= 0.3
thr= 2.8
L1 = 21.6
h1 = 1.5
theta1 = 0.122454045649174
L2 = 21.6
h2 = 1.45
theta2 = 0.0355872634481644
Lr = 80
```

```
hr = 6
thetar = 0.0378212848907171
swidth=9.8
sheight=83.8

Wvb= 2.989  !Width of the vertical resistive beams
Lvb= 16    !Length of the vertical resistive beams
Whb= 4.416  !Width of the horizontal resistive beam
Lhb= 265.0281    !Length of the horizontal resistive beam

Ey = 164000
Pr = 0.23
NLegs=2
dY = -10
rho = 11.7e-8  !Resistivity (n-type Si)
p11=-40.9e-5   !-102.2e-5
p12=27.4e-5   !53.4e-5
p44=0  !-13.6e-5

Vs=1.5
Vg=0
/NOPR

ET,1,PLANE223,101

R,1,t
R,2,tvr
R,3,thr
MP,EX,1,Ey     !*** Youngs Modulus ***
MP,PRXY,1,Pr   !*** Poisson's Ratio ***
MP,RSVX,1,rho
```

```
TB,PZRS,1
TBDATA,1,P11,P12,P12
TBDATA,7,P12,P11,P12
TBDATA,13,P12,P12,P11
TBDATA,22,P44

Nonlinear = 1
Steps = 16
!=============================================================
!            RELATIONAL PARAMETERS
!=============================================================

Lx=L1*cos(theta1)+Lr*cos(thetar)+L2*cos(theta2)
Ly=L1*sin(theta1)+Lr*sin(thetar)+L2*sin(theta2)

!=============================================================
!            MODEL SETUP
!=============================================================
K,3,0,0,0
K,4,0,h1/(2*sin(PI/2-theta1)),0
K,5,0,-h1/(2*sin(PI/2-theta1)),0
K,8,L1*cos(theta1)-h1/2*sin(theta1),L1*sin(theta1)+h1/2*cos(theta1),0
K,9,L1*cos(theta1),L1*sin(theta1),0
K,10,L1*cos(theta1)+h1/2*sin(theta1),L1*sin(theta1)-h1/2*cos(theta1),0
K,11,L1*cos(theta1)-hr/2*sin(thetar),L1*sin(theta1)+hr/2*cos(thetar),0
K,12,L1*cos(theta1)+Lr*cos(thetar)-hr/2*sin(thetar),L1*sin(theta1)+Lr*sin(thetar)+hr/
        2*cos(thetar),0
K,13,L1*cos(theta1)+Lr*cos(thetar)-h2/2*sin(theta2),L1*sin(theta1)+Lr*sin(thetar)+h2/
        2*cos(theta2),0
K,14,L1*cos(theta1)+Lr*cos(thetar),L1*sin(theta1)+Lr*sin(thetar),0
```

```
K,15,L1*cos(theta1)+Lr*cos(thetar)+h2/2*sin(theta2),L1*sin(theta1)+Lr*sin(thetar)-h2/
      2*cos(theta2),0
K,16,L1*cos(theta1)+Lr*cos(thetar)+hr/2*sin(thetar),L1*sin(theta1)+Lr*sin(thetar)-hr/
      2*cos(thetar),0
K,17,L1*cos(theta1)+hr/2*sin(thetar),L1*sin(theta1)-hr/2*cos(thetar),0
K,18,Lx,Ly,0
K,19,Lx,Ly+h2/(2*sin(PI/2-theta2)),0
K,20,Lx,Ly+sheight/Nlegs/2,0
K,21,Lx+swidth/2,Ly+sheight/Nlegs/2,0
K,22,Lx+swidth/2,Ly-sheight/Nlegs/2,0
K,23,Lx,Ly-sheight/Nlegs/2,0
K,24,Lx,Ly-h2/(2*sin(PI/2-theta2)),0

L,4,8
L,8,11
L,11,12
L,12,13
L,13,19
L,19,20
L,20,21
L,21,22
L,22,23
L,23,24
L,24,15
L,15,16
L,16,17
L,17,10
L,10,5
L,5,4
LFILLT,1,2,h1
LFILLT,14,15,h1
```

```
LFILLT,4,5,h2
LFILLT,5,6,h2
LFILLT,10,11,h2
LFILLT,11,12,h2

AL,ALL
AGEN,Nlegs,1,1,1,0,-sheight/Nlegs,0,0,0,0
ARSYM,X,ALL,0,0,0
AGEN,2,Nlegs+1,2*Nlegs,1,Lx+swidth/2,0,0,0,0,1
AGEN,2,Nlegs+1,2*Nlegs,1,Lx+swidth/2,0,0,0,0,1
AADD,ALL

K,200,-5,-sheight/2,0    !Create 1st Vertical Beam Resistor
K,201,-5-Wvb,-sheight/2,0
K,202,-5-Wvb,-sheight/2-Lvb,0
K,203,-5,-sheight/2-Lvb,0
L,200,201
L,201,202
L,202,203
L,203,200
AL,8,9,31,32

K,204,2*Lx+swidth+5,-sheight/2,0!Create 2nd Vertical Beam Resistor
K,205,2*Lx+swidth+5+Wvb,-sheight/2,0
K,206,2*Lx+swidth+5+Wvb,-sheight/2-Lvb,0
K,207,2*Lx+swidth+5,-sheight/2-Lvb,0
L,204,205
L,205,206
L,206,207
L,207,204
AL,33,54,55,56
```

```
K,300,0,-sheight-20,0
K,301,0,-sheight-20-Whb,0
K,302,Lhb,-sheight-20-Whb,0
K,303,Lhb,-sheight-20,0
L,300,301
L,301,302
L,302,303
L,303,300
AL,75,76,77,78

!*** MESH MECHANISM ***
real,1
type,1
mat,1

AESIZE,5,h1/3
AMESH,5

!*** MESH VERTICAL BEAM RESISTORS ***
real,2
type,1
mat,1

AESIZE,1,wvb/3
AESIZE,2,wvb/3
AMESH,1,2,1

!*** MESH HORIZONTAL BEAM RESISTOR ***
real,3
type,1
```

```
mat,1

AESIZE,3,whb/3
AMESH,3

!*** Get Node Number at KeyPoint 21 ***
ksel,s,kp,,21
nslk,s
*get,nkp1,node,0,num,max
nsel,all
ksel,all

!============ Electrical Boundary Contraints  =============

LSEL,S,LINE,,16        !Define supply voltage contact
LSEL,A,LINE,,44
LSEL,A,LINE,,8
NSLL,S,1
CP,1,VOLT,ALL
*GET,ns,NODE,0,NUM,MIN
D,NS,VOLT,Vs

LSEL,S,LINE,,55       !Define ground contact
LSEL,A,LINE,,77
NSLL,S,1
CP,2,VOLT,ALL
*GET,ng,NODE,0,NUM,MIN
D,NG,VOLT,0

LSEL,S,LINE,,31        !Define first output contact
LSEL,A,LINE,,75
```

```
NSLL,S,1
CP,3,VOLT,ALL
*GET,no1,NODE,00,NUM,MIN

LSEL,S,LINE,,66        !Define second output contact
LSEL,A,LINE,,88
LSEL,A,LINE,,33
NSLL,S,1
CP,4,VOLT,ALL
*GET,no2,NODE,0,NUM,MIN
NSEL,ALL
LSEL,ALL

!========== Structural Boundary Constraints ==========

DL,16,,UX,0
DL,16,,UY,0
DL,44,,UX,0
DL,44,,UY,0
DL,66,,UX,0
DL,66,,UY,0
DL,88,,UX,0
DL,88,,UY,0

DK,21,UY,-dY
FINISH

!=====================================================
!              SOLUTION STEPS
!=====================================================
/SOLU
```

```
NLGEOM,1       !***Nonlinear Analysis****
ANTYPE,0       !***Static Analysis Type***

!============ VERTICAL DISPLACEMENT =============
*DO,mm,1,Steps+1,1
  DK,21, ,(mm-1)*dY/Steps, , , ,UY, , , , ,
  lswrite,mm
*ENDDO

lssolve,1,Steps+1

FINISH

/POST1

!=========== RETRIEVE IMPORTANT DATA ===

*DIM,Smax,TABLE,Steps+1
*DIM,Ydis,TABLE,Steps+1
*DIM,Force,TABLE,Steps+1
*DIM,VoltO1,TABLE,Steps+1
*DIM,VoltO2,TABLE,Steps+1
*DO,n,1,Steps+1,1
Set,n

ETABLE,svonm,S,EQV

ESORT,ETAB,svonm,0,1
*GET,Smax(n),SORT,0,MAX
```

```
*GET,Ydis(n),NODE,nkp1,U,Y

*GET,Force(n),NODE,nkp1,RF,FY

*GET,VoltO1(n),NODE,no1,VOLT
*GET,VoltO2(n),NODE,no2,VOLT

*ENDDO

!Create Output File

/output,Configuration_C_results.txt
*VWRITE
YdisYforceSmaxVoltO1VoltO2
*VWRITE,Ydis(1),Force(1),Smax(1),VoltO1(1),VoltO2(1)
%15e %15e %15e %15e %15e
/output

FINISH
```

Configuration D

```
!=============================================================
!  Created by Jeff Anderson, 20 Jun 05
!  This batch file uses 8-Node Coupled-Field Solid elements to analyze the piezoresistivity
        of a Fully
!  Compliant Bistable Mechanism.
!  Config D- see thesis for configuration description
!
!=============================================================
/TITLE,Analysis of a Fully Compliant Bistable Mechanism
/CLEAR,NOSTART
```

```
/PREP7
PI=acos(-1)
!=============================================================
!              INPUT PARAMETERS
!=============================================================
t = 4.75
tr= 0.3
L1 = 21.6
h1 = 1.5
theta1 = 0.122454045649174
L2 = 21.6
h2 = 1.45
theta2 = 0.0355872634481644
Lr = 80
hr = 6
thetar = 0.0378212848907171
swidth=9.8
sheight=83.8

Wb= 2.989  !Width of the resistive beam
Lb= 16    !Length of the resistive beam

Ey = 164000
Pr = 0.23
NLegs=2
dY = -10
rho = 11.7e-8  !Resistivity (n-type Si)
p11=-102.2e-5
p12=53.4e-5
p44=-13.6e-5
```

```
Vs=1.5
Vg=0
/NOPR

ET,1,PLANE223,101

R,1,t
R,2,tr
MP,EX,1,Ey     !*** Youngs Modulus ***
MP,PRXY,1,Pr   !*** Poisson's Ratio ***
MP,RSVX,1,rho

TB,PZRS,1
TBDATA,1,P11,P12,P12
TBDATA,7,P12,P11,P12
TBDATA,13,P12,P12,P11
TBDATA,22,P44

Nonlinear = 1
Steps = 16
!=========================================================
!              RELATIONAL PARAMETERS
!=========================================================

Lx=L1*cos(theta1)+Lr*cos(thetar)+L2*cos(theta2)
Ly=L1*sin(theta1)+Lr*sin(thetar)+L2*sin(theta2)

!=========================================================
!              MODEL SETUP
!=========================================================
K,3,0,0,0
```

```
K,4,0,h1/(2*sin(PI/2-theta1)),0
K,5,0,-h1/(2*sin(PI/2-theta1)),0
K,8,L1*cos(theta1)-h1/2*sin(theta1),L1*sin(theta1)+h1/2*cos(theta1),0
K,9,L1*cos(theta1),L1*sin(theta1),0
K,10,L1*cos(theta1)+h1/2*sin(theta1),L1*sin(theta1)-h1/2*cos(theta1),0
K,11,L1*cos(theta1)-hr/2*sin(thetar),L1*sin(theta1)+hr/2*cos(thetar),0
K,12,L1*cos(theta1)+Lr*cos(thetar)-hr/2*sin(thetar),L1*sin(theta1)+Lr*sin(thetar)+hr/
     2*cos(thetar),0
K,13,L1*cos(theta1)+Lr*cos(thetar)-h2/2*sin(theta2),L1*sin(theta1)+Lr*sin(thetar)+h2/
     2*cos(theta2),0
K,14,L1*cos(theta1)+Lr*cos(thetar),L1*sin(theta1)+Lr*sin(thetar),0
K,15,L1*cos(theta1)+Lr*cos(thetar)+h2/2*sin(theta2),L1*sin(theta1)+Lr*sin(thetar)-h2/
     2*cos(theta2),0
K,16,L1*cos(theta1)+Lr*cos(thetar)+hr/2*sin(thetar),L1*sin(theta1)+Lr*sin(thetar)-hr/
     2*cos(thetar),0
K,17,L1*cos(theta1)+hr/2*sin(thetar),L1*sin(theta1)-hr/2*cos(thetar),0
K,18,Lx,Ly,0
K,19,Lx,Ly+h2/(2*sin(PI/2-theta2)),0
K,20,Lx,Ly+sheight/Nlegs/2,0
K,21,Lx+swidth/2,Ly+sheight/Nlegs/2,0
K,22,Lx+swidth/2,Ly-sheight/Nlegs/2,0
K,23,Lx,Ly-sheight/Nlegs/2,0
K,24,Lx,Ly-h2/(2*sin(PI/2-theta2)),0

L,4,8
L,8,11
L,11,12
L,12,13
L,13,19
L,19,20
L,20,21
```

```
L,21,22
L,22,23
L,23,24
L,24,15
L,15,16
L,16,17
L,17,10
L,10,5
L,5,4
LFILLT,1,2,h1
LFILLT,14,15,h1
LFILLT,4,5,h2
LFILLT,5,6,h2
LFILLT,10,11,h2
LFILLT,11,12,h2

AL,ALL
AGEN,Nlegs,1,1,1,0,-sheight/Nlegs,0,0,0,0
ARSYM,X,ALL,0,0,0
AGEN,2,Nlegs+1,2*Nlegs,1,Lx+swidth/2,0,0,0,0,1
AGEN,2,Nlegs+1,2*Nlegs,1,Lx+swidth/2,0,0,0,0,1
AADD,ALL

AGEN,2,5,5,1,0,-sheight-20,0,0,0,0      !Create second bistable mechanism


K,200,-5,-sheight/2,0    !Create 1st Beam Resistor
K,201,-5-Wb,-sheight/2,0
K,202,-5-Wb,-sheight/2-Lb,0
K,203,-5,-sheight/2-Lb,0
L,200,201
```

```
L,201,202
L,202,203
L,203,200
AL,161,162,163,164

K,204,2*Lx+swidth+5,-sheight/2,0
K,205,2*Lx+swidth+5+Wb,-sheight/2,0
K,206,2*Lx+swidth+5+Wb,-sheight/2-Lb,0
K,207,2*Lx+swidth+5,-sheight/2-Lb,0
L,204,205
L,205,206
L,206,207
L,207,204
AL,165,166,167,168

!*** MESH MECHANISMS ***
real,1
type,1
mat,1

AESIZE,5,h1/3
AESIZE,1,h1/3
AMESH,5
AMESH,1

!*** MESH BEAM RESISTORS ***
real,2
type,1
mat,1

AESIZE,2,wb/3
```

```
AESIZE,3,wb/3
AMESH,2,3,1

!*** Get Node Number at KeyPoint 21 ***
ksel,s,kp,,21
nslk,s
*get,nkp1,node,0,num,max
nsel,all
ksel,all

!============ Electrical Boundary Contraints  =============

LSEL,S,LINE,,16        !Define supply voltage contact
LSEL,A,LINE,,44
LSEL,A,LINE,,161
NSLL,S,1
CP,1,VOLT,ALL
*GET,ns,NODE,0,NUM,MIN
D,NS,VOLT,Vs

LSEL,S,LINE,,167       !Define ground contact
LSEL,A,LINE,,139
LSEL,A,LINE,,158
NSLL,S,1
CP,2,VOLT,ALL
*GET,ng,NODE,0,NUM,MIN
D,NG,VOLT,0

LSEL,S,LINE,,163        !Define first output contact
LSEL,A,LINE,,118
LSEL,A,LINE,,99
```

```
NSLL,S,1
CP,3,VOLT,ALL
*GET,no1,NODE,00,NUM,MIN

LSEL,S,LINE,,66        !Define second output contact
LSEL,A,LINE,,88
LSEL,A,LINE,,165
NSLL,S,1
CP,4,VOLT,ALL
*GET,no2,NODE,0,NUM,MIN
NSEL,ALL
LSEL,ALL

!=========== Structural Boundary Constraints ==========

DL,16,,UX,0
DL,16,,UY,0
DL,44,,UX,0
DL,44,,UY,0
DL,66,,UX,0
DL,66,,UY,0
DL,88,,UX,0
DL,88,,UY,0
DL,118,,UX,0
DL,118,,UY,0
DL,99,,UX,0
DL,99,,UY,0
DL,139,,UX,0
DL,139,,UY,0
DL,158,,UX,0
DL,158,,UY,0
```

```
DK,21,UY,-dY
FINISH

!=========================================================
!             SOLUTION STEPS
!=========================================================
/SOLU

NLGEOM,1       !***Nonlinear Analysis****
ANTYPE,0       !***Static Analysis Type***

!============ VERTICAL DISPLACEMENT =============
*DO,mm,1,Steps+1,1
  DK,21, ,(mm-1)*dY/Steps, , , ,UY, , , , ,
  lswrite,mm
*ENDDO

lssolve,1,Steps+1

FINISH

/POST1

!=========== RETRIEVE IMPORTANT DATA ===

*DIM,Smax,TABLE,Steps+1
*DIM,Ydis,TABLE,Steps+1
*DIM,Force,TABLE,Steps+1
*DIM,VoltO1,TABLE,Steps+1
*DIM,VoltO2,TABLE,Steps+1
```

```
*DO,n,1,Steps+1,1
Set,n

ETABLE,svonm,S,EQV

ESORT,ETAB,svonm,0,1
*GET,Smax(n),SORT,0,MAX

*GET,Ydis(n),NODE,nkp1,U,Y

*GET,Force(n),NODE,nkp1,RF,FY

*GET,VoltO1(n),NODE,no1,VOLT
*GET,VoltO2(n),NODE,no2,VOLT
*ENDDO

!Create Output File

/output,Configuration_D_results.txt
*VWRITE
YdisYforceSmaxVoltO1VoltO2
*VWRITE,Ydis(1),Force(1),Smax(1),VoltO1(1),VoltO2(1)
%15e %15e %15e %15e %15e
/output

FINISH
```